

1
2
3
4
5
6
7
8
9
10
11
12
13
14
15
16
17
18
19
20
21
22
23
24
25
26
27
28
29
30
31
32
33
34
35
36
37
38
39
40
41
42
43
44
45
46
47

Golgi-localized exo- β 1,3-galactosidases involved in AGP modification and root cell expansion in Arabidopsis

Pieter Nibbering¹, Bent L. Petersen², Mohammed Saddik Motawia², Bodil Jørgensen², Peter Ulvskov², Totte Niittylä^{1*}

¹Department of Forest Genetics and Plant Physiology, Umeå Plant Science Centre, Swedish University of Agricultural Sciences, 901 83 UMEÅ

²Department of Plant and Environmental Sciences, University of Copenhagen, DK-1871 Frederiksberg C, Denmark

*corresponding author: Totte Niittylä, totte.niittyla@slu.se

48 **Abstract**

49 Plant arabinogalactan proteins (AGPs) are a diverse group of cell surface- and wall-associated
50 glycoproteins. Functionally important AGP glycans are synthesized in the Golgi apparatus,
51 but the relationships between their glycosylation, processing, and functionality are poorly
52 understood. Here we report the identification and functional characterization of two Golgi-
53 localized $\text{exo-}\beta\text{-1,3-galactosidases}$ from the glycosyl hydrolase 43 (GH43) family in
54 *Arabidopsis thaliana*. *GH43* loss of function mutants exhibit root cell expansion defects in
55 sugar-containing growth media. This root phenotype is associated with an increase in the
56 extent of AGP cell wall association, as demonstrated by Yariv phenylglycoside dye
57 quantification and comprehensive microarray polymer profiling of sequentially extracted cell
58 walls. Recombinant GH43 characterization showed that the $\text{exo-}\beta\text{-1,3-galactosidase}$ activity
59 of GH43s is hindered by $\beta\text{-1,6}$ branches on $\beta\text{-1,3-galactans}$. In line with this steric hindrance,
60 the recombinant GH43s did not release galactose from cell wall extracted glycoproteins or
61 AGP rich gum arabic. These results show that *Arabidopsis* GH43s are involved in AGP
62 glycan biosynthesis in the Golgi, and suggest their $\text{exo-}\beta\text{-1,3-galactosidase}$ activity influences
63 AGP and cell wall matrix interactions, thereby adjusting cell wall extensibility.

64

65

66

67

68

69

70

71

72

73

74

75

76

77

78

79 **Introduction**

80 Plant cell growth is dictated by turgor-driven extension of the primary cell wall. Oriented
81 cellulose biosynthesis and localised wall deposition create dynamic cell wall mechanics that
82 enable turgor-driven anisotropic cell growth (Cosgrove, 2005). Studies on the molecular
83 interactions in the primary cell wall matrix have led to models in which covalent and non-
84 covalent interactions between matrix components facilitate anisotropic cell expansion
85 (Bashline et al., 2014). The primary cell wall polysaccharide matrix contains cellulose,
86 hemicellulose and pectin as well as enzymes and structural proteins (Ellis et al., 2010; Harholt
87 et al., 2010; Rose and Lee, 2010; Scheller and Ulvskov, 2010). The cell wall-associated
88 glycoproteins include arabinogalactan proteins (AGPs), which are proposed to have diverse
89 roles during cell expansion, including as structural components, modifiers of the extracellular
90 matrix, and ligands for cell surface receptors (Showalter et al., 2010; Xue et al., 2017).

91
92 Glycans account for 90-98% of the molecular weight of AGPs, and are thought to be critical
93 for their functionality (Showalter, 1993). Characterisation of the enzymes responsible for
94 AGP glycosylation can elucidate AGP functions and functional redundancies (Showalter et
95 al., 2010; Showalter and Basu, 2016). AGP glycosylation is initiated by proline hydroxylation
96 in the ER and is then advanced in the Golgi apparatus by specialized glycosyl transferases
97 (GTs) (Rose and Lee, 2010; Hijazi et al., 2014). The glycosyl transferase family 31 (GT31) is
98 responsible for the synthesis of the hydroxyproline galactose and the β -1,3-galactan backbone
99 of AGPs (Basu et al., 2015; Basu et al., 2015; Ogawa-Ohnishi and Matsubayashi, 2015;
100 Suzuki et al., 2017). Defects in β -1,3-galactan biosynthesis are associated with various
101 developmental phenotypes including defects in cell expansion (Basu et al., 2015; Ogawa-
102 Ohnishi and Matsubayashi, 2015; Suzuki et al., 2017). The side chains, which branch off from
103 the β -1,3-galactan back bone via β -1,6 linkages, are synthesized by GALT29A and/or GT31
104 family enzymes (Geshi et al., 2013; Dilokpimol et al., 2014). Further side chain residues are
105 attached by other GTs: GT77 enzymes add α -1,3/1,5-arabinose units (Gille et al., 2013), by
106 GT14 attaches β -1,6 glucuronic acid units (Knoch et al., 2013; Dilokpimol et al., 2014), and
107 GT37 adds α -1,2-fucose units (Wu et al., 2010; Tryfona et al., 2014). These GTs acting on
108 AGPs are expected to generate a glycan structure consisting of a β -1,3 galactan backbone
109 with β -1,6 galactan branches containing diverse other sugars.

110
111 Despite the advances in identifying GTs involved in AGP glycosylation, the *in vivo* structural
112 diversity of mature arabinogalactans is huge and largely uncharacterised. The glycan structure

113 is also likely to vary between AGPs, tissues, and even cell types, as indicated by differences
114 in extractability, expression during specific growth stages, and the expression of the
115 glycosylation machinery (Pennell et al., 1991; Showalter et al., 2010). Nuclear magnetic
116 resonance (NMR) analysis of the glycans attached to synthetic AGP motif repeats expressed
117 in tobacco Bright Yellow-2 cells revealed relatively short galactan backbone with a mixture of
118 β -1,6 and β -1,3 links (Tan et al., 2004; Tan et al., 2010). The side chains were also short and
119 contained a mixture of galactose, arabinose, glucuronic acid, and rhamnose. How well these
120 structures reflect native structures is unclear. Larger glycans were found in radish roots, wheat
121 flowers, and *Arabidopsis* leaves based on mass spectrometric analysis of enzymatically
122 released AGP glycans (Haque et al., 2005; Tryfona et al., 2010; Tryfona et al., 2012). The
123 evidence from these structural glycan studies and characterizations of GTs active on AGPs
124 suggest a β -1,3 galactan backbone of varying length with β -1,6 side chains containing mainly
125 galactan and arabinose residues with some additional sugar residues also found in pectin.

126

127 We hypothesize that hydrolytic enzymes acting on AGP glycans may also be involved in the
128 synthesis of the arabinogalactan chains or their modification in the cell wall matrix. There is
129 precedent for apoplastic post-deposition modification of xyloglucan by hydrolases (Gunl et
130 al., 2011; Gunl and Pauly, 2011), but secretory pathway modification as known from N-
131 glycan biosynthesis should also be considered. Based on the description of hydrolase enzymes
132 in the carbohydrate-active enzyme database (CAZy), glycoside hydrolase family 43 (GH43)
133 was identified as a potential group with AGP glycan hydrolyzing activity (Kotake et al., 2009;
134 Geshi et al., 2013; Mewis et al., 2016). The GH43 family is conserved across prokaryotes and
135 eukaryotes; it currently contains 15 620 GH43 enzymes, making it one of the largest known
136 hydrolase families. The family is divided into α -L-arabinofuranosidase, β -D-xylosidase, α -L-
137 arabinanase, and β -D-galactosidase groups (Mewis et al., 2016). Several GH43 enzymes from
138 prokaryotes and eukaryotes have recently been characterized because of their potential in
139 biomass degradation and other biotechnological applications (Jordan et al., 2013; McCleary et
140 al., 2015). Based on their diverse identified enzymatic activities and amino acid motifs, the
141 GH43s have been further subdivided into 37 subclades (Mewis et al., 2016). However, no
142 GH43 family enzyme from plants has yet been characterized. The *Arabidopsis thaliana*
143 genome contains two genes encoding amino acid sequences with similarity to GH43 enzymes
144 belonging to the GH43 subfamily 24, named GH43A and GH43B (Mewis et al., 2016). Here,
145 we characterize these GH43 enzymes and describe their role in cell expansion and root
146 growth in *Arabidopsis thaliana*.

147 **Results**

148

149 ***GH43* null mutants are defective in cell expansion**

150 The *Arabidopsis thaliana* genome encodes two putative glycosyl hydrolase 43 family
151 enzymes according to the latest version of the *Arabidopsis* Information Resource database
152 (TAIR; <https://www.arabidopsis.org/>). Based on publicly available expression data, both
153 genes are expressed throughout plant development with high expression in roots and stems.
154 To investigate the functional role of these GH43 enzymes, we first obtained mutants carrying
155 exon T-DNA insertions in *GH43A* and *GH43B* (Fig 1a). Initial analysis of the single *gh43*
156 mutants and the double *gh43a-1/gh43b-1* mutant (*gh43null* henceforth) revealed no obvious
157 visual phenotypes in seedlings or mature plants (Fig 1b and Supplemental Fig 1). Since *GH43*
158 genes are expressed in seedlings and young roots according to publicly available expression
159 data (eFP browser: <http://bar.utoronto.ca/>), we focused our subsequent phenotyping on
160 seedlings grown on nutrient media agar plates.

161

162 Several classic cell wall mutants in *Arabidopsis* show enhanced or conditional root growth
163 defects on media containing 4.5 % exogenous sugar (Benfey et al., 1993; Hauser et al.,
164 1995). We therefore grew the *gh43* mutants on nutrient media without sugar for four days and
165 then moved them to media containing 4.5 % glucose for six days. During the six days on
166 glucose media, the *gh43a* and WT roots elongated at similar rates. However, root growth was
167 slightly reduced in the *gh43b-1* and *gh43b-2* single mutants, and severely inhibited in
168 *gh43null* (Fig 1c, and 1d). No change in growth rate was observed in controls moved to media
169 without sugar (Fig 1e). On sugar-containing media, the *gh43null* root epidermal cells
170 exhibited clear swelling and loss of anisotropic growth (Fig 1f). A time course experiment
171 comparing WT and *gh43null* lines expressing the plasma membrane marker LTI6a-GFP
172 revealed that the swelling was detectable in the cell elongation zone already after 6 hours and
173 became obvious after 10 hours (Fig 1g and Supplemental Fig 2). This cell expansion defect is
174 not observed on media containing 4.5 % sorbitol or 100 mM NaCl, showing that the
175 phenotype cannot be caused by an osmotic effect alone or salt stress (Supplemental Fig 3). To
176 confirm the causal gene defect responsible for the sugar-inducible loss of anisotropic growth,
177 we performed complementation experiments by introducing either *GH43A-cYFP* or the
178 *GH43B-cYFP* under the control of their native promoters into *gh43null* background. Both
179 constructs rescued the root growth phenotype (Fig 1d).

180

181 **GH43A and GH43B are Golgi localized β -1,3-galactosidases**

182 The *pGH43A:GH43A-cYFP* and *pGH43B:GH43B-cYFP* lines were used to investigate the
183 subcellular location of the GH43s. In the expanding root cells of four-day old seedlings, both
184 GH43A-cYFP and GH43B-cYFP appeared to localize to the Golgi apparatus (Fig 2a). To
185 confirm the Golgi localisation, the lines were crossed with lines carrying the *cis*-Golgi marker
186 SYP32-mCherry or the *trans*-Golgi network marker SYP43-mCherry (Fig 2a) (Uemura et al.,
187 2004; Geldner et al., 2009). Both GH43 proteins co-localised with the Golgi markers. The
188 overlap with SYP32-mCherry was higher than that with SYP43-mCherry, indicating a slight
189 enrichment in the *cis*-Golgi (Fig 2b and 2c). In further support of the Golgi localisation, both
190 Arabidopsis GH43s were identified in Golgi-enriched cell extracts in global proteomics
191 experiments (Parsons et al., 2012; Parsons et al., 2019).

192
193 The predicted hydrolase domains of the two Arabidopsis GH43 proteins exhibit over 90 %
194 similarity at the amino acid sequence level, suggesting similar enzyme activity (Supplemental
195 Fig 4). Sequence similarity also indicates that these proteins belong to the GH43 subfamily of
196 enzymes with β -1,3-galactosidase activity (Ichinose et al., 2005; Ichinose et al., 2006; Kotake
197 et al., 2009; Jiang et al., 2012; Mewis et al., 2016). To test for this activity, we expressed
198 GH43A and GH43B in *Escherichia coli* and purified the recombinant proteins using nickel
199 ion affinity chromatography (Supplemental Fig 5a). The activity of the recombinant GH43s
200 was assayed against various of β -1,3-galactan di- and trisaccharides (Fig 3). Both GH43
201 proteins hydrolysed β -D-Galp-(1 \rightarrow 3)- β -D-GalpOMe, but not β -D-Galp-(1 \rightarrow 6)- β -D-GalpOMe.
202 To confirm that the observed β -1,3-galactosidase activity was due to the GH43 enzymes, we
203 generated GH43 enzymes with mutations in the predicted active site. The mutation sites were
204 selected based on sequence similarity with the active site of a *Clostridium thermocellum*
205 GH43 protein whose structure was solved by crystallography (Supplemental Fig 5b) (Jiang et
206 al., 2012). Of the mutated versions, the GH43B^{EQ224} had minor activity towards β -D-Galp-
207 (1 \rightarrow 3)- β -D-GalpOMe, while GH43B^{EQ224,338} and GH43B^{337-339DEL} were inactive towards β -D-
208 Galp-(1 \rightarrow 3)- β -D-GalpOMe (Supplemental Fig 5c). These assays confirmed that the
209 Arabidopsis GH43s are β -1,3-galactosidases and support the conservation of active sites
210 between bacteria and plants.

211
212 β -1,3-galactan in plant cell walls is mainly found on AGPs (Du et al., 1996). Therefore, to
213 investigate the presence of possible GH43 substrates in Arabidopsis cell walls, we
214 sequentially extracted cell wall glycoproteins from Arabidopsis leaves using 0.2M CaCl₂, 50

215 mM CDTA, 0.5M NaCO₃, and 4M NaOH, and analysed the extracts by thin layer
216 chromatography (TLC) before and after treatment with the GH43 proteins (Supplemental Fig
217 6a). Interestingly, the recombinant GH43s did not release galactose from any of the cell wall
218 fractions, suggesting that the β -1,3-linkages were inaccessible. The recombinant GH43s also
219 failed to release galactose from Gum Arabic, which is rich in AGPs (Supplemental Fig 6b)
220 (Akiyama et al., 1984). Even partial deglycosylation of the AGPs was insufficient to allow the
221 GH43 proteins access to the β -1,3-linkages (Supplemental Fig 6b). These observations
222 suggested that the β -1,3-linkages of mature AGPs may be protected against GH43 activity.

223

224 To investigate the enzymatic mechanism of the Arabidopsis GH43 proteins in more depth, we
225 synthesized β -1,3 galactan oligosaccharides with a β -1,6-galactose branch on the reducing and
226 non-reducing ends of β -D-Galp-(1 \rightarrow 3)- β -D-GalpOMe. The GH43s were unable to hydrolyze
227 the β -D-Galp-(1 \rightarrow 3)- β -D-GalpOMe when the non-reducing end bore a β -1,6-galactose unit,
228 but did hydrolyze it when the substitution was at the reducing end (Fig 3). Steric hindrance
229 due to the presence of side chains at the non-reducing end of the β -1,3 galactan thus protects
230 against hydrolysis catalysed by GH43 proteins. We also tested the ability of GH43s to
231 hydrolyse β -1,3- or β -1,4-glucans, but observed no activity towards these polymers
232 (Supplemental Fig 6c). These localisation and recombinant enzyme assays established the two
233 Arabidopsis GH43s as Golgi exo- β -1,3 galactosidases with quite strict substrate specificity.

234

235 ***gh43* null mutants have altered cell wall structure**

236 WT and *gh43null* seedlings had similar contents of cellulose, hemicellulosic and pectic sugars
237 (Supplemental Fig 7, Supplemental Table 1). The *gh43null* root swelling thus cannot be
238 explained by changes in the levels of the main cell wall polymers, although it is possible that
239 more localized cell-type specific defects were masked by the analysis of total tissue extracts.
240 Based on the GH43 proteins' Golgi localisation, exo- β 1,3-galactosidase activity and inactivity
241 towards AGP-containing plant extracts, we hypothesised that they are involved in the
242 synthesis of the arabinogalactans in the Golgi. It is plausible that their native targets occur
243 only found in the Golgi and represent a small fraction of the total β -1,3-galactan pool. This
244 hypothesis is consistent with the inactivity of the GH43 proteins towards β -1,3 galactans
245 substituted with a β -1,6 galactan at the non-reducing end, and suggests that GH43s may be
246 involved in the processing of the AGPs during biosynthesis.

247

248 We hypothesised that defects in arabinogalactan synthesis in the *gh43null* background would
249 cause changes in the structure and/or extractability of AGPs. To investigate this possibility,
250 we first quantified the levels of cell wall-bound AGPs (isolated by removing the CaCl₂-
251 soluble fraction followed by AIR1 treatment) and AGPs soluble in 0.18 M CaCl₂ in WT and
252 *gh43null* seedlings using β -Yariv. Yariv phenyl glycosides selectively bind to the β -1,3
253 galactans of AGPs, enabling their spectrophotometric quantification (Kitazawa et al., 2013).
254 The fraction of cell wall-bound AGPs in *gh43null* was higher than in the WT (Fig 4a), where
255 as a tendency for the opposite was observed for the soluble fraction (Fig 4b). We thus
256 hypothesized that structural differences in the AGP glycans of the *gh43null* mutant may cause
257 some AGPs to bind more tightly to the cell wall.

258
259 AGPs bound to cell walls may affect matrix properties and conceivably also cell expansion.
260 To test whether this could explain the root swelling phenotype, we sequentially extracted cell
261 wall fractions from 7-day old WT and *gh43null* seedlings using 180 mM CaCl₂, 50 mM
262 CDTA, and 4 M NaOH/26.5 mM NaBH₄. Equal amount of each fraction was analysed on a
263 Comprehensive Microarray Polymer Profiling (CoMPP) microarray designed to determine
264 different sugar epitopes in complex plant extracts (Moller et al., 2012). Similar polymer
265 profiling has also previously been employed to demonstrate cell wall matrix separability
266 features (Harholt et al., 2012; Tan et al., 2013). The CoMPP microarray contained
267 monoclonal antibodies specific for pectin, xylan, xyloglucan, mannan, crystalline cellulose,
268 extensin and AGP epitopes (Supplemental Table 2). For epitopes released with 180mM
269 CaCl₂, the JIM13, LM20 and RU2 antibody signals of *gh43null* were significantly weaker
270 than those of the WT (Table I). Pectin antibodies LM20 and RU2 bind partially
271 methylesterified homogalacturonan and the rhamnogalacturonan-I (RG-I) backbone,
272 respectively (Verhertbruggen et al., 2009; Ralet et al., 2010), while JIM13 recognises an AGP
273 epitope (Yates et al., 1996). For epitopes released with 50 mM CDTA, the LM5, LM15 and
274 LM18 signals of the *gh43null* were significantly stronger than those of the WT (Table I).
275 Pectin epitope antibody LM5 binds to β 1,4-galactan, LM18 to partially methylesterified
276 homogalacturonan, and LM15 to xyloglucan (Jones et al., 1997; Marcus et al., 2008;
277 Verhertbruggen et al., 2009). The cell wall fraction exhibiting the most pronounced
278 differences between *gh43null* and WT was the extracted with 4 M NaOH/26.5 mM NaBH₄
279 released epitopes (Table I). In accordance with the β -Yariv assay results (Fig 4a), the signals
280 from the AGP antibodies JIM13, LM2, LM14 and MAC207 were all significantly more
281 intense in *gh43null* (Table I) (Smallwood et al., 1996; Yates et al., 1996; Ruprecht et al.,

282 2017). An increased signal intensity in *gh43null* was also observed for the pectin (galactan)
283 antibody LM5, the xyloglucan binding LM25, and the CBM3a crystalline cellulose and
284 JIM20 extensin antibodies (Smallwood et al., 1994; Verhertbruggen et al., 2009; Hernandez-
285 Gomez et al., 2015). These CoMPP results established that the defect caused by the loss of
286 GH43 β -1,3-galactosidase activity causes changes in the abundance of cell wall-associated
287 AGPs.

288

289 **Discussion**

290 β 1,3-galactan in plant cell walls is found primarily on AGPs (Du et al., 1996). We identified
291 and characterized the enzymatic activity of two Golgi-localized GH43 exo- β 1,3-
292 galactosidases and discovered that their activity influences the levels of cell wall associated
293 AGPs. Functional characterisation of plant GH43 enzymes has not previously been reported.
294 The active site of the prokaryotic GH43 from *Clostridium thermocellum* and the Arabidopsis
295 GH43s is conserved (Supplemental Fig 5). Despite this catalytic similarity, the Arabidopsis
296 GH43s are involved in cell wall biosynthesis whereas their prokaryotic and fungal
297 counterparts are involved in plant cell wall degradation (Ichinose et al., 2005; Ichinose et al.,
298 2006; Kotake et al., 2009; Jiang et al., 2012; Mewis et al., 2016). The functional role of GH43
299 activity during root growth was revealed by experiments using nutrient media supplemented
300 with 4.5% glucose. On such media, root growth is modestly reduced in single *gh43b* mutants
301 and dramatically reduced in the *gh43null* double mutant (Fig 1). Nutrient media with 4.5%
302 sugar was also used in a classical genetic screen for conditional root growth mutants of
303 Arabidopsis (Benfey et al. 1993; Hauser et al. 1995). Several mutants identified in this way
304 were subsequently shown to be defective in cell wall biosynthesis genes including the
305 glycosylphosphatidylinositol-anchored plasma membrane protein *COBRA* (Schindelman et
306 al., 2001), the chitinase-like protein *CTL1* (Sanchez-Rodriguez et al., 2012) and the cellulose
307 synthase interacting 1 (*CSII*) (Gu et al., 2010). The mechanism responsible for the sugar-
308 induced root growth defects in these cell wall mutants and the *gh43* mutants remains unclear,
309 but may involve cell wall acidification of sugar-activated proton pumps and/or disturbance of
310 hormone homeostasis (Niittyta et al., 2007; Ljung et al., 2015; Yeats et al., 2016). The root
311 cell expansion defects of *gh43null* become noticeable in the elongation zone within 6 hours of
312 transferring seedlings to sugar media (Supplementary Fig 2). Quantification of cell wall-
313 associated AGPs with β -Yariv (Fig 4), and the CoMPP analysis of cell wall fractions from
314 untreated seedlings (Table I) confirmed that the *gh43null* cell walls differ from WT even

315 before the sugar treatment. Thus, a pre-existing cell wall defect is likely to underlie the sugar
316 induced swelling.

317

318 Investigation of the *gh43null* cell wall defect revealed a connection to AGPs. We observed
319 AGP epitopes in all sequentially extracted cell wall fractions (Table I). The increase in the
320 levels of AGPs extracted from the *gh43null* with 4 M NaOH (i.e. AGPs not released by
321 180mM CaCl₂ or 50mM CDTA) suggests that GH43s play a role in adjusting the cell wall
322 affinity of AGPs. The CoMPP microarray analysis of cell wall fractions also revealed subtle
323 differences in the abundance of pectin and xyloglucan epitopes in the *gh43null* mutant (Table
324 I). We hypothesise that these changes reflect modifications of the cell wall matrix resulting
325 from initial changes in the AGPs. Based on the inactivity of GH43s towards β -1,3 galactans
326 with β -1,6 branching (Fig 3), and the lack of galactose release from extracted cell wall
327 glycoproteins or AGP-rich gum arabic (Supplemental Fig 6), we propose that the Arabidopsis
328 GH43s are required for β -1,3-galactan processing during AGP maturation in the Golgi. It is
329 conceivable that GH43s regulate the length of the β -1,3-galactan backbone (and thus the
330 number of side chains that can attach to it), and/or modify the backbone length to make it
331 accessible to other enzymes. The Golgi-associated α -mannosidase I, which is involved in
332 structuring N-glycosylation, has been demonstrated to perform proteoglycan trimming of this
333 sort in Arabidopsis (Liebminger et al., 2009). A similar AGP glycan structuring role could be
334 envisaged for GH43s.

335

336 Accumulating evidence from several plant species supports the existence of cell wall matrix-
337 bound AGPs, primarily associated with pectin (summarised by Tan et al. (2013)). Pectin can
338 be subdivided into homogalacturonan (HG), xylogalacturonan (XGA), apiogalacturonan,
339 rhamnogalacturonan type I (RG-I), and rhamnogalacturonan type II (RG-II) (Harholt et al.,
340 2010). Of these, HG and RG-I are the most abundant in Arabidopsis primary walls,
341 accounting for ~65% and 20-35% of the total pectin content, respectively (Mohnen, 2008).
342 HG is a linear α -1,4-linked galacturonic acid that is partially methylesterified and can be O-
343 acetylated. RG-I consists of a α -1,4-D-galacturonic acid- α -1,2-L-rhamnose backbone with
344 several side chains (Harholt et al., 2010). The RG-I side chains include galactans and
345 arabinans as well as arabinogalactan type I (AG-I), and arabinogalactan type II (AG-II)
346 polysaccharide chains (Yapo, 2011). The AG-II structure resembles that of AGP glycans and
347 it may be that some of the RG-I attached oligosaccharides actually derive from AGP glycans.
348 In Arabidopsis, the AGP ARABINOXYLAN PECTIN ARABINO GALACTAN PROTEIN1

349 (APAP1) binds covalently to RG-I/HG and was shown to increase the extractability of pectin
350 and hemicellulosic immunoreactive epitopes, suggesting that it acts as a structural cross-linker
351 in plant cell walls for this AGP (Tan et al., 2013). Whether the covalent bond between APAP1
352 and RG-I is a result of transglycosylation taking place in the apoplast or synthesises as such in
353 the Golgi is unknown. Interestingly, the CoMPP microarray results for the *gh43null* mutant
354 revealed decreased homogalacturonan (LM20) and RGI-backbone (RU2) signals in the CaCl₂
355 soluble fraction, and increased β -1,4-galactan (LM5) and homogalacturonan (LM18) signal in
356 the CDTA fraction and β -1,4-galactan (LM5) in the NaOH fraction (Table I). Together, these
357 results show that *gh43null* exhibits altered pectin extractability compared with the WT, and
358 suggest that APAP1 and/or similar cell wall-bound AGPs could be targets of GH43 activity.

359

360 Pectin in expanding cells has been proposed to function as a mechanical tether between
361 cellulose microfibrils (Höfte et al., 2012), and as a lubricant of microfibril movement during
362 cell expansion (Cosgrove, 2014). Experimental support for direct interaction between
363 cellulose and pectin in primary cell walls of Arabidopsis was provided by the comparison of
364 never dried, dehydrated and rehydrated cell walls using multidimensional solid state nuclear
365 magnetic resonance (NMR) spectroscopy (Wang et al. (2015). The NMR spectra showed
366 cross peaks between cellulose and pectin indicating that some of the pectic sugars come into
367 subnanometer contact with cellulose microfibrils. Based on these pectin models, AGP and
368 pectin interactions would be expected to influence primary cell wall extensibility by
369 restricting cellulose microfibril movement and/or cell wall matrix extension. This concept was
370 first introduced in an early cell wall model proposed in the 1970s, which depicted covalent
371 connections between pectin and structural proteins (Keegstra et al., 1973). However, strong
372 evidence of the role of structural cell wall proteins has been slow to emerge and therefore
373 many current cell wall models omit them. The involvement of GH43s in the modification of
374 AGP association with cell walls breathes new life into the concept of structural cell wall
375 proteins, and establishes a previously unknown β -1,3-galactan trimming process during
376 primary plant cell biosynthesis and cell growth. Cell wall bound AGPs may play an
377 important role as structural matrix proteins preventing cellulose microfibril coalescence,
378 simultaneously hindering other cell wall polymers from binding to cellulose. In this model,
379 more tightly bound AGPs could impair wall stiffening during cell expansion, and thus
380 contribute to the *gh43null* root swelling phenotype. This interpretation would imply that the
381 distribution, measured as extractability, of other polymers in the wall would also change and
382 this seems indeed to be the case in the *gh43null* mutant.

383

384

385 **Methods**

386

387 **Plant material and growth conditions**

388 *gh43a-1* (GABI_062D83), *gh43b-1* (Salk_002830), *gh43b-2* (SALK_087519) were ordered
389 from NASC and genotyped (Supplemental table 3). The T-DNA insert locations were
390 determined by sequencing (Fig 1a). Mutant and wild type plants were grown on soil at 22 °C
391 with a photoperiod of 16 h light and 8 h dark at 65% relative humidity.

392

393 **Plant vector construction and transformation**

394 The genomic sequences of GH43A and B were amplified using the primers in Supplemental
395 Table 3. The amplified pieces were cloned in the pDONR207 plasmid via Gibson assembly
396 and recombined into pHGY (Kubo et al., 2005). Both constructs were transformed into
397 *gh43null*. Stably transgenic plants were generated by *Agrobacterium tumefaciens*-mediated
398 transformation. Transgenic seedlings were selected based on hypocotyl elongation on 0.9%
399 agar ½ MS plates supplemented with 30 µg/mL hygromycin. Homozygous lines were
400 generated based on hygromycin segregation and detection of the YFP signal by confocal
401 microscopy.

402

403 **Root elongation/complementation experiments**

404 Seeds were surface sterilized with 70% ethanol and grown on ½ MS agar plates (0.9% agar, 5
405 mM MES, pH 5.7) for 4 days. After this period, the seedlings were moved to ½ MS plates, ½
406 MS plates containing either 4.5% glucose or 4.5% sorbitol or 100 mM NaCl plates. The
407 seedlings were then allowed to grow for 6 days. The difference in root elongation from day 0
408 on the new plate to day 6 was quantified using Image J (<https://imagej.nih.gov/ij/>).

409

410 **GH43 protein localization and root imaging in the LTi6a-GFP background**

411 The lines *pGH43A::GH43A-cYFP* and *pGH43B::GH43B-cYFP* co-expressing the marker
412 lines SYP32-mCherry or SYP43-mCherry were generated by plant crossing (Uemura et al.,
413 2004; Geldner et al., 2009). For observation, seedlings were grown vertically on plates
414 containing ½ MS media with 0.9% plant agar for 5 days and then observed under a Zeiss
415 LSM880 confocal laser scanning microscope. A Zeiss LSM880 confocal laser scanning

416 microscope with an Airyscan detector and a LD LCI Plan-Apochromat 40x/1.2 Imm
417 AutoCorr DIC M27 water immersion objective was used.

418 The *LTI6a-GFP* line was crossed in the *gh43null* mutant background and homozygous lines
419 were generated (Grebe et al., 2003). The seedlings were grown for 4 days on ½ MS plates and
420 then moved to ½ MS plates or ½ MS plates with 4.5% glucose. The roots were imaged with a
421 Zeiss LSM880 confocal microscope.

422

423 **Heterologous expression and purification of the GH43 proteins**

424 The *Arabidopsis* GH43 coding sequences were amplified from 121-1401 bp (AT5G67540.1,
425 GH43A) and 115-1401 bp (AT3G49880, GH43B) to avoid the predicted membrane domain.
426 The proteins were expressed in Rosettatm (DE3) *E.coli* cells using a pET24d His10SUMO
427 vector. The crude protein extract was purified by Ni-NTA, then the His10SUMO tag was
428 cleaved and the GH43 protein isolated by Ni-NTA chromatography (Supplemental Fig 5a).

429

430 **Synthesis of methyl β-D- Galactopyranoside substrates 1-4 (Fig 3).**

431 Chemical synthesis of methyl 3-O-β-D-galactopyranosyl-β-D-galactopyranoside (1) (Kovac et
432 al., 1985), methyl 6-O-β-D-galactopyranosyl-β-D-galactopyranoside (2) (Kovac et al., 1984),
433 and methyl 3,6-di-O-(β-D-galactopyranosyl)-β-D-galactopyranoside (4) (Kaji et al., 2010)
434 have been reported in literature. However, methyl β-D-galactopyranosyl-(1→6)-β-D-
435 galactopyranosyl-(1→3)-β-D-galactopyranoside (3) has not previously been reported. The
436 strategy for chemical synthesis of the substrates 1-4 is outlined in Supplemental Fig 8

437

438 **GH43 protein activity assays**

439 The enzymes' buffer was changed to 10 mM MOPS (pH 7) using the PD SpintrapTM G-25
440 (GE Healthcare, 28-9180-04) protocol. To determine the activity towards the β-galactan
441 substrates (Fig 4) and β-glucan substrates (Supplemental Fig 6C), 1 μg GH43A and 4 μg
442 GH43B were incubated with 100 μg of substrate (15 μl total volume), overnight at 30 °C
443 while shaking. For tests using the inactive enzymes, 1 μg was loaded (Supplemental Fig 5c).
444 Gum Arabic (200 mg/ml) was hydrolysed in 0.1 M TFA hydrolysed at 80 °C for 45 minutes
445 (loading 10 μl on a TLC plate). The TFA was then removed using a speed vac by reducing the
446 reaction mixture's volume to around half of its original value. 30 mg of the resulting digestion
447 product was further hydrolysed with an enzyme cocktail containing 1μl β-galactanase (E-
448 BGLAN), 0.5μl β-glucuronosidase (E-BGLAEC), 18μl α-Fucosidase (E-FUCTM) and 20μl

449 α -Arabinofuranosidase (E-ABFAN) from Megazyme in a 50 mM sodium acetate buffer pH5
450 at 37 °C for 4 hours (again, 10 μ l was loaded on a TLC plate). The enzymes were then
451 inactivated at 95 °C for 15 minutes, after which their buffer was changed to 10 mM MOPS
452 (pH 7) using a PD MidiTrap G-10 column to 10mM MOPS pH7 to remove the sodium acetate
453 and digestion products. The total sample was incubated with 2.5 μ g GH43A or 10 μ g of
454 GH43B overnight while shaking at 30°C, then concentrated with a speed vac to
455 approximately 10 μ l and loaded onto a TLC plate.

456 Sequentially extracted cell wall material (10 mg/100 μ l MOPS pH 7) was incubated with 2 μ g
457 GH43A or 7.5 μ g of GH43B at 30 °C overnight while shaking. The samples were then
458 concentrated with a speed vac to approximately 10 μ l and loaded onto a TLC plate.

459 The products were loaded on a TLC Silica Gel 60 F254 TLC plate membrane and developed
460 with 4:1:1 (1-Butanol:Acetic acid: H₂O). The membranes were visualized with 5 %
461 Sulphuric acid and 0.5 % Thymol in 96 % ethanol at 105°C.

462

463 **AGP quantification with β -Yariv**

464 Soluble AGP purification and quantification was performed according to Lamport (2013). For
465 quantification of cell wall-associated AGPs, the cell wall pellet left after the removing CaCl₂-
466 soluble AGPs was flash frozen in liquid nitrogen and then lyophilized. The resulting material
467 was ball milled, AIR1-treated (see below) and lyophilized. The lyophilized material was then
468 incubated with β -Yariv for 4 hours at room temperature, and the β -Yariv absorbance was
469 spectrophotometrically quantified according to Lamport (2013).

470

471 **Sequential extraction and Comprehensive Microarray Polymer Profiling (CoMPP)**

472 Seeds were surface sterilized with 70 % ethanol and grown on ½ MS agar plates (0.9% agar, 5
473 mM MES, pH 5.7) for 7 days. The seedlings were then harvested, flash frozen, and ground in
474 liquid nitrogen with a mortar and pestle. CaCl₂-soluble glycoproteins were extracted with 0.18
475 M CaCl₂ (2ml/g fresh weight) for 2 hours at RT and spun down at 4000g×10min. The pellet
476 containing the cell wall material was freeze dried, ball milled, and AIR1-treated (see below)
477 before further processing. The supernatant was precipitated with 4 volumes of ethanol at 4 °C
478 for 16 hours and spun down at 2000g×2min. The pellet was further solubilized in 45 mM
479 CaCl₂ (2 ml/g fresh weight from starting material) and freeze dried. For the carbohydrate
480 microarray, the soluble glycoproteins and cell wall material were further treated and analysed
481 according to Moller et al. (2012). For determination of the monosugar composition, the
482 fractions extracted with 50 mM CDTA and 4M NaOH/ 26.5mM NaBH₄ fractions were
483 dialysed against demineralised water using Visking® 12-14 kD dialysis tubing (45 mm).

484
485 **Wet chemical analysis of cell walls**

486 The 7-day old seedlings were harvested, flash frozen and lyophilized. The dried material was
487 ball milled, and the alcohol-insoluble residue (AIR1) was removed by incubating the material
488 first for 30 minutes in 80% ethanol, and then for 30 minutes in 70 % ethanol at 95 °C, and
489 finally in chloroform:methanol (1 : 1) for 5 min at room temperature before washing with
490 acetone. This sequence of incubations and washes constitutes the AIR1 treatment mentioned
491 above. Starch (AIR2) was then removed according to Rende et al. (2016). The mono sugar
492 composition was measured according to Latha Gandla et al. (2015). The crystalline cellulose
493 content was quantified according to the Updegraff (1969).

494
495
496 **Supplemental data**

497
498 **Supplementary Table 1.** Hemicellulosic/pectin sugar composition of sequential extracted
499 cell wall fractions of 7-day old Col-0 and *gh43null* seedlings.

500 **Supplementary Table 2.** Binding specificity of the CoMPP antibodies

501 **Supplementary Table 3.** Primers used for genotyping the *gh43* lines and cloning of the
502 *GH43-cYFP* constructs.

503 **Supplementary Figure S1.** Picture of ten-week-old *Col-0* and *gh43* lines.

504 **Supplementary Figure 2.** Confocal laser scanning microscope images of Col-0 and *gh43null*
505 roots stably expressing the LTI6a-GFP plasma membrane marker.

506 **Supplementary Figure 3.** Col-0 and the *gh43* grown on 4.5% sorbitol or 100mM NaCl.

507 **Supplementary Figure 4.** Amino acid sequence alignment of GH43A and GH43B.

508 **Supplementary Figure 5.** Activity of heterologous expressed GH43B proteins with
509 mutations in predicted active site.

510 **Supplementary Figure 6.** Activity of the heterologous expressed GH43 proteins towards
511 Gum Arabic, partially digested Gum Arabic, sequentially extracted cell wall material and β 1,3
512 or β 1,4 glucan substrates.

513 **Supplementary Figure 7.** Crystalline cellulose content in 7-day old Col-0 and the *gh43null*
514 seedlings.

515 **Supplementary Figure 8.** Chemical synthesis of the methyl β -galactopyronosides.

516

517 **Acknowledgements**

518 We would like to thank Mikael Lindberg from the Umeå University Protein Expertise
519 Platform (PEP), for help with expressing the recombinant Arabidopsis GH43s. We would like
520 to thank Dr. Junko Takahashi-Schmidt and the UPSC Biopolymer Analytical Platform for
521 help with the cell wall monosugar analysis. This work was supported by The Swedish
522 Foundation for Strategic Research (Value Tree), Bio4Energy (Swedish Programme for
523 Renewable Energy), the UPSC Centre for Forest Biotechnology funded by VINNOVA and
524 the Swedish Research Council for Sustainable Development (Formas).

525

526

527 **Author Contribution**

528 P.N., B.P., M.S.M., B.J. and P.U. planned and performed experiments and analyzed data. T.N.
529 planned experiments and analyzed data. P.N. and T.N. wrote the manuscript with help from
530 the other authors.

531

532

533 **Literature**

534

535 Akiyama Y, Eda S, Kato K (1984) Gum Arabic Is a Kind of Arabinogalactan Protein. *Agricultural and*
536 *Biological Chemistry* 48: 235-237

537 Bashline L, Lei L, Li SD, Gu Y (2014) Cell Wall, Cytoskeleton, and Cell Expansion in Higher Plants.
538 *Molecular Plant* 7: 586-600

539 Basu D, Tian L, Wang W, Bobbs S, Herock H, Travers A, Showalter AM (2015) A small multigene
540 hydroxyproline-O-galactosyltransferase family functions in arabinogalactan-protein
541 glycosylation, growth and development in Arabidopsis. *BMC Plant Biol* 15: 295

542 Basu D, Wang W, Ma S, DeBrosse T, Poirier E, Emch K, Soukup E, Tian L, Showalter AM (2015) Two
543 Hydroxyproline Galactosyltransferases, GALT5 and GALT2, Function in Arabinogalactan-
544 Protein Glycosylation, Growth and Development in Arabidopsis. *PLoS One* 10: e0125624

545 Benfey PN, Linstead PJ, Roberts K, Schiefelbein JW, Hauser MT, Aeschbacher RA (1993) Root
546 development in Arabidopsis: four mutants with dramatically altered root morphogenesis.
547 *Development* 119: 57-70

548 Cosgrove DJ (2005) Growth of the plant cell wall. *Nat Rev Mol Cell Biol* 6: 850-861

549 Cosgrove DJ (2014) Re-constructing our models of cellulose and primary cell wall assembly. *Current*
550 *Opinion in Plant Biology* 22: 122-131

551 Dilokpimol A, Poulsen CP, Vereb G, Kaneko S, Schulz A, Geshi N (2014) Galactosyltransferases from
552 Arabidopsis thaliana in the biosynthesis of type II arabinogalactan: molecular interaction
553 enhances enzyme activity. *BMC Plant Biol* 14: 90

554 Du H, Clarke AE, Bacic A (1996) Arabinogalactan-proteins: a class of extracellular matrix
555 proteoglycans involved in plant growth and development. *Trends Cell Biol* 6: 411-414

556 Ellis M, Egelund J, Schultz CJ, Bacic A (2010) Arabinogalactan-proteins: key regulators at the cell
557 surface? *Plant Physiol* 153: 403-419

558 Geldner N, Denervaud-Tendon V, Hyman DL, Mayer U, Stierhof YD, Chory J (2009) Rapid,
559 combinatorial analysis of membrane compartments in intact plants with a multicolor marker
560 set. *Plant Journal* 59: 169-178

561 Geshi N, Johansen JN, Dilokpimol A, Rolland A, Belcram K, Verger S, Kotake T, Tsumuraya Y, Kaneko S,
562 Tryfona T, Dupree P, Scheller HV, Hofte H, Mouille G (2013) A galactosyltransferase acting on
563 arabinogalactan protein glycans is essential for embryo development in Arabidopsis. *Plant*
564 *Journal* 76: 128-137

565 Gille S, Sharma V, Baidoo EEK, Keasling JD, Scheller HV, Pauly M (2013) Arabinosylation of a Yariv-
566 Precipitable Cell Wall Polymer Impacts Plant Growth as Exemplified by the Arabidopsis
567 Glycosyltransferase Mutant ray1. *Molecular Plant* 6: 1369-1372

568 Grebe M, Xu J, Mobius W, Ueda T, Nakano A, Geuze HJ, Rook MB, Scheres B (2003) Arabidopsis sterol
569 endocytosis involves actin-mediated trafficking via ARA6-positive early endosomes. *Curr Biol*
570 13: 1378-1387

571 Gu Y, Kaplinsky N, Bringmann M, Cobb A, Carroll A, Sampathkumar A, Baskin TI, Persson S, Somerville
572 CR (2010) Identification of a cellulose synthase-associated protein required for cellulose
573 biosynthesis. *Proceedings of the National Academy of Sciences of the United States of*
574 *America* 107: 12866-12871

- 575 Gunl M, Neumetzler L, Kraemer F, de Souza A, Schultink A, Pena M, York WS, Pauly M (2011) AX18
576 encodes an alpha-fucosidase, underscoring the importance of apoplastic metabolism on the
577 fine structure of Arabidopsis cell wall polysaccharides. *Plant Cell* 23: 4025-4040
- 578 Gunl M, Pauly M (2011) AX13 encodes a alpha-xylosidase that impacts the structure and accessibility
579 of the hemicellulose xyloglucan in Arabidopsis plant cell walls. *Planta* 233: 707-719
- 580 Haque M, Kotake T, Tsumuraya Y (2005) Mode of action of beta-glucuronidase from *Aspergillus niger*
581 on the sugar chains of arabinogalactan-protein. *Biosci Biotechnol Biochem* 69: 2170-2177
- 582 Harholt J, Sorensen I, Fangel J, Roberts A, Willats WGT, Scheller HV, Petersen BL, Banks A, Ulvskov P
583 (2012) The Glycosyltransferase Repertoire of the Spikemoss *Selaginella moellendorffii* and a
584 Comparative Study of Its Cell Wall. *Plos One* 7
- 585 Harholt J, Suttangkakul A, Vibe Scheller H (2010) Biosynthesis of pectin. *Plant Physiol* 153: 384-395
- 586 Hauser MT, Morikami A, Benfey PN (1995) Conditional root expansion mutants of Arabidopsis.
587 *Development* 121: 1237-1252
- 588 Hernandez-Gomez MC, Rydahl MG, Rogowski A, Morland C, Cartmell A, Crouch L, Labourel A, Fontes
589 CM, Willats WG, Gilbert HJ, Knox JP (2015) Recognition of xyloglucan by the crystalline
590 cellulose-binding site of a family 3a carbohydrate-binding module. *FEBS Lett* 589: 2297-2303
- 591 Hijazi M, Velasquez SM, Jamet E, Estevez JM, Albenne C (2014) An update on post-translational
592 modifications of hydroxyproline-rich glycoproteins: toward a model highlighting their
593 contribution to plant cell wall architecture. *Front Plant Sci* 5: 395
- 594 Höfte H, Peaucelle A, Braybrook S (2012) Cell wall mechanics and growth control in plants: the role of
595 pectins revisited. *Frontiers in plant science* 3: 121
- 596 Ichinose H, Kuno A, Kotake T, Yoshida M, Sakka K, Hirabayashi J, Tsumuraya Y, Kaneko S (2006)
597 Characterization of an exo-beta-1,3-galactanase from *Clostridium thermocellum*. *Appl*
598 *Environ Microbiol* 72: 3515-3523
- 599 Ichinose H, Yoshida M, Kotake T, Kuno A, Igarashi K, Tsumuraya Y, Samejima M, Hirabayashi J,
600 Kobayashi H, Kaneko S (2005) An exo-beta-1,3-galactanase having a novel beta-1,3-galactan-
601 binding module from *Phanerochaete chrysosporium*. *J Biol Chem* 280: 25820-25829
- 602 Jiang D, Fan J, Wang X, Zhao Y, Huang B, Liu J, Zhang XC (2012) Crystal structure of 1,3Gal43A, an exo-
603 beta-1,3-galactanase from *Clostridium thermocellum*. *J Struct Biol* 180: 447-457
- 604 Jones L, Seymour GB, Knox JP (1997) Localization of pectic galactan in tomato cell walls using a
605 monoclonal antibody specific to (1->4)-beta-D-galactan. *Plant Physiology* 113: 1405-1412
- 606 Jordan DB, Wagschal K, Grigorescu AA, Braker JD (2013) Highly active beta-xylosidases of glycoside
607 hydrolase family 43 operating on natural and artificial substrates. *Appl Microbiol Biotechnol*
608 97: 4415-4428
- 609 Keegstra K, Talmadge KW, Bauer W, Albersheim P (1973) The structure of plant cell walls: III. A model
610 of the walls of suspension-cultured sycamore cells based on the interconnections of the
611 macromolecular components. *Plant physiology* 51: 188-197
- 612 Kitazawa K, Tryfona T, Yoshimi Y, Hayashi Y, Kawauchi S, Antonov L, Tanaka H, Takahashi T, Kaneko S,
613 Dupree P, Tsumuraya Y, Kotake T (2013) beta-galactosyl Yariv reagent binds to the beta-1,3-
614 galactan of arabinogalactan proteins. *Plant Physiol* 161: 1117-1126
- 615 Knoch E, Dilokpimol A, Tryfona T, Poulsen CP, Xiong GY, Harholt J, Petersen BL, Ulvskov P, Hadi MZ,
616 Kotake T, Tsumuraya Y, Pauly M, Dupree P, Geshi N (2013) A beta-glucuronosyltransferase
617 from Arabidopsis thaliana involved in biosynthesis of type II arabinogalactan has a role in cell
618 elongation during seedling growth. *Plant Journal* 76: 1016-1029
- 619 Kotake T, Kitazawa K, Takata R, Okabe K, Ichinose H, Kaneko S, Tsumuraya Y (2009) Molecular cloning
620 and expression in *Pichia pastoris* of a *Irpex lacteus* exo-beta-(1->3)-galactanase gene. *Biosci*
621 *Biotechnol Biochem* 73: 2303-2309
- 622 Kubo M, Udagawa M, Nishikubo N, Horiguchi G, Yamaguchi M, Ito J, Mimura T, Fukuda H, Demura T
623 (2005) Transcription switches for protoxylem and metaxylem vessel formation. *Genes Dev*
624 19: 1855-1860
- 625 Lamport DT (2013) Preparation of arabinogalactan glycoproteins from plant tissue. *Bioprotocol* 3: 1-5

- 626 Latha Gandla M, Derba-Maceluch M, Liu X, Gerber L, Master ER, Mellerowicz EJ, Jonsson LJ (2015)
627 Expression of a fungal glucuronoyl esterase in *Populus*: effects on wood properties and
628 saccharification efficiency. *Phytochemistry* 112: 210-220
- 629 Liebminger E, Huttner S, Vavra U, Fischl R, Schoberer J, Grass J, Blaukopf C, Seifert GJ, Altmann F,
630 Mach L, Strasser R (2009) Class I alpha-mannosidases are required for N-glycan processing
631 and root development in *Arabidopsis thaliana*. *Plant Cell* 21: 3850-3867
- 632 Ljung K, Nemhauser JL, Perata P (2015) New mechanistic links between sugar and hormone signalling
633 networks. *Current Opinion in Plant Biology* 25: 130-137
- 634 Marcus SE, Verhertbruggen Y, Herve C, Ordaz-Ortiz JJ, Farkas V, Pedersen HL, Willats WG, Knox JP
635 (2008) Pectic homogalacturonan masks abundant sets of xyloglucan epitopes in plant cell
636 walls. *BMC Plant Biol* 8: 60
- 637 McCleary BV, McKie VA, Draga A, Rooney E, Mangan D, Larkin J (2015) Hydrolysis of wheat flour
638 arabinoxylan, acid-debranched wheat flour arabinoxylan and arabino-xylo-oligosaccharides
639 by beta-xylanase, alpha-L-arabinofuranosidase and beta-xylosidase. *Carbohydr Res* 407: 79-
640 96
- 641 Mewis K, Lenfant N, Lombard V, Henrissat B (2016) Dividing the Large Glycoside Hydrolase Family 43
642 into Subfamilies: a Motivation for Detailed Enzyme Characterization. *Appl Environ Microbiol*
643 82: 1686-1692
- 644 Mohnen D (2008) Pectin structure and biosynthesis. *Curr Opin Plant Biol* 11: 266-277
- 645 Moller IE, Pettolino FA, Hart C, Lampugnani ER, Willats WGT, Bacic A (2012) Glycan Profiling of Plant
646 Cell Wall Polymers using Microarrays. *Jove-Journal of Visualized Experiments*
- 647 Niittyla T, Fuglsang AT, Palmgren MG, Frommer WB, Schulze WX (2007) Temporal analysis of sucrose-
648 induced phosphorylation changes in plasma membrane proteins of *Arabidopsis*. *Mol Cell*
649 *Proteomics* 6: 1711-1726
- 650 Ogawa-Ohnishi M, Matsubayashi Y (2015) Identification of three potent hydroxyproline O-
651 galactosyltransferases in *Arabidopsis*. *Plant J* 81: 736-746
- 652 Parsons HT, Christiansen K, Knierim B, Carroll A, Ito J, Batth TS, Smith-Moritz AM, Morrison S,
653 McInerney P, Hadi MZ, Auer M, Mukhopadhyay A, Petzold CJ, Scheller HV, Loque D,
654 Heazlewood JL (2012) Isolation and proteomic characterization of the *Arabidopsis* Golgi
655 defines functional and novel components involved in plant cell wall biosynthesis. *Plant*
656 *Physiol* 159: 12-26
- 657 Parsons HT, Stevens TJ, McFarlane HE, Vidal-Melgosa S, Griss J, Lawrence N, Butler R, Sousa MML,
658 Salemi M, Willats WGT, Petzold CJ, Heazlewood JL, Lilley KS (2019) Separating Golgi proteins
659 from cis to trans reveals underlying properties of cisternal localization. *Plant Cell*
- 660 Pennell RI, Janniche L, Kjellbom P, Scofield GN, Peart JM, Roberts K (1991) Developmental Regulation
661 of a Plasma-Membrane Arabinogalactan Protein Epitope in Oilseed Rape Flowers. *Plant Cell*
662 3: 1317-1326
- 663 Ralet MC, Tranquet O, Poulain D, Moise A, Guillon F (2010) Monoclonal antibodies to
664 rhamnogalacturonan I backbone. *Planta* 231: 1373-1383
- 665 Rende U, Wang W, Gandla ML, Jonsson LJ, Niittyla T (2016) Cytosolic invertase contributes to the
666 supply of substrate for cellulose biosynthesis in developing wood. *New Phytol*
- 667 Rose JKC, Lee SJ (2010) Straying off the Highway: Trafficking of Secreted Plant Proteins and
668 Complexity in the Plant Cell Wall Proteome. *Plant Physiology* 153: 433-436
- 669 Ruprecht C, Bartetzko MP, Senf D, Dallabernadina P, Boos I, Andersen MCF, Kotake T, Knox JP, Hahn
670 MG, Clausen MH, Pfrenkle F (2017) A Synthetic Glycan Microarray Enables Epitope Mapping
671 of Plant Cell Wall Glycan-Directed Antibodies. *Plant Physiol* 175: 1094-1104
- 672 Sanchez-Rodriguez C, Bauer S, Hematy K, Saxe F, Ibanez AB, Vodermaier V, Konlechner C,
673 Sampathkumar A, Ruggeberg M, Aichinger E, Neumetzler L, Burgert I, Somerville C, Hauser
674 MT, Persson S (2012) Chitinase-like1/pom-pom1 and its homolog CTL2 are glucan-interacting
675 proteins important for cellulose biosynthesis in *Arabidopsis*. *Plant Cell* 24: 589-607
- 676 Scheller HV, Ulvskov P (2010) Hemicelluloses. *Annu Rev Plant Biol* 61: 263-289

- 677 Schindelman G, Morikami A, Jung J, Baskin TI, Carpita NC, Derbyshire P, McCann MC, Benfey PN
678 (2001) COBRA encodes a putative GPI-anchored protein, which is polarly localized and
679 necessary for oriented cell expansion in Arabidopsis. *Genes & development* 15: 1115-1127
- 680 Showalter AM (1993) Structure and function of plant cell wall proteins. *Plant Cell* 5: 9-23
- 681 Showalter AM, Basu D (2016) Extensin and Arabinogalactan-Protein Biosynthesis:
682 Glycosyltransferases, Research Challenges, and Biosensors. *Front Plant Sci* 7: 814
- 683 Showalter AM, Keppler B, Lichtenberg J, Gu D, Welch LR (2010) A bioinformatics approach to the
684 identification, classification, and analysis of hydroxyproline-rich glycoproteins. *Plant Physiol*
685 153: 485-513
- 686 Smallwood M, Beven A, Donovan N, Neill SJ, Peart J, Roberts K, Knox JP (1994) Localization of Cell-
687 Wall Proteins in Relation to the Developmental Anatomy of the Carrot Root Apex. *Plant*
688 *Journal* 5: 237-246
- 689 Smallwood M, Yates EA, Willats WGT, Martin H, Knox JP (1996) Immunochemical comparison of
690 membrane-associated and secreted arabinogalactan-proteins in rice and carrot. *Planta* 198:
691 452-459
- 692 Suzuki T, Narciso JO, Zeng W, van de Meene A, Yasutomi M, Takemura S, Lampugnani ER, Doblin MS,
693 Bacic A, Ishiguro S (2017) KNS4/UPEX1: A Type II Arabinogalactan beta-(1,3)-
694 Galactosyltransferase Required for Pollen Exine Development. *Plant Physiol* 173: 183-205
- 695 Tan L, Eberhard S, Pattathil S, Warder C, Glushka J, Yuan C, Hao Z, Zhu X, Avci U, Miller JS, Baldwin D,
696 Pham C, Orlando R, Darvill A, Hahn MG, Kieliszewski MJ, Mohnen D (2013) An Arabidopsis
697 cell wall proteoglycan consists of pectin and arabinoxylan covalently linked to an
698 arabinogalactan protein. *Plant Cell* 25: 270-287
- 699 Tan L, Qiu F, Lamport DTA, Kieliszewski MJ (2004) Structure of a hydroxyproline (Hyp)-
700 arabinogalactan polysaccharide from repetitive Ala-Hyp expressed in transgenic *Nicotiana*
701 *tabacum*. *Journal of Biological Chemistry* 279: 13156-13165
- 702 Tan L, Varnai P, Lamport DT, Yuan C, Xu J, Qiu F, Kieliszewski MJ (2010) Plant O-hydroxyproline
703 arabinogalactans are composed of repeating trigalactosyl subunits with short bifurcated side
704 chains. *J Biol Chem* 285: 24575-24583
- 705 Tryfona T, Liang HC, Kotake T, Kaneko S, Marsh J, Ichinose H, Lovegrove A, Tsumuraya Y, Shewry PR,
706 Stephens E, Dupree P (2010) Carbohydrate structural analysis of wheat flour arabinogalactan
707 protein. *Carbohydrate Research* 345: 2648-2656
- 708 Tryfona T, Liang HC, Kotake T, Tsumuraya Y, Stephens E, Dupree P (2012) Structural characterization
709 of Arabidopsis leaf arabinogalactan polysaccharides. *Plant Physiol* 160: 653-666
- 710 Tryfona T, Theys TE, Wagner T, Stott K, Keegstra K, Dupree P (2014) Characterisation of FUT4 and
711 FUT6 alpha-(1 -> 2)-Fucosyltransferases Reveals that Absence of Root Arabinogalactan
712 Fucosylation Increases Arabidopsis Root Growth Salt Sensitivity. *Plos One* 9
- 713 Uemura T, Ueda T, Ohniwa RL, Nakano A, Takeyasu K, Sato MH (2004) Systematic analysis of SNARE
714 molecules in Arabidopsis: dissection of the post-Golgi network in plant cells. *Cell Struct Funct*
715 29: 49-65
- 716 Updegraff DM (1969) Semimicro determination of cellulose in biological materials. *Anal Biochem* 32:
717 420-424
- 718 Verhertbruggen Y, Marcus SE, Haeger A, Ordaz-Ortiz JJ, Knox JP (2009) An extended set of
719 monoclonal antibodies to pectic homogalacturonan. *Carbohydr Res* 344: 1858-1862
- 720 Wang T, Park YB, Cosgrove DJ, Hong M (2015) Cellulose-Pectin Spatial Contacts Are Inherent to
721 Never-Dried Arabidopsis Primary Cell Walls: Evidence from Solid-State Nuclear Magnetic
722 Resonance. *Plant Physiol* 168: 871-884
- 723 Wu Y, Williams M, Bernard S, Driouich A, Showalter AM, Faik A (2010) Functional identification of
724 two nonredundant Arabidopsis alpha(1,2)fucosyltransferases specific to arabinogalactan
725 proteins. *J Biol Chem* 285: 13638-13645
- 726 Xue H, Veit C, Abas L, Tryfona T, Maresch D, Ricardi MM, Estevez JM, Strasser R, Seifert GJ (2017)
727 Arabidopsis thaliana FLA 4 functions as a glycan-stabilized soluble factor via its carboxy-
728 proximal Fasciclin 1 domain. *The Plant Journal* 91: 613-630

- 729 Yapo BM (2011) Rhamnogalacturonan-I: a structurally puzzling and functionally versatile
730 polysaccharide from plant cell walls and mucilages. *Polymer Reviews* 51: 391-413
- 731 Yates EA, Valdor JF, Haslam SM, Morris HR, Dell A, Mackie W, Knox JP (1996) Characterization of
732 carbohydrate structural features recognized by anti-arabinogalactan-protein monoclonal
733 antibodies. *Glycobiology* 6: 131-139
- 734 Yeats TH, Sorek H, Wemmer DE, Somerville CR (2016) Cellulose Deficiency Is Enhanced on Hyper
735 Accumulation of Sucrose by a H⁺-Coupled Sucrose Symporter. *Plant Physiology* 171: 110-124
- 736
- 737

738

Table I. Comprehensive Microarray Polymer Profiling (CoMPP) of sequentially extracted cell walls from seven-day old Col-0 and *gh43null* seedlings.

Cell wall fractions extracted with 180mM CaCl₂, 50 mM cyclohexanediamine tetraacetic acid (CDTA) and 4M NaOH/26.5mM NaBH₄. The values represent the signal intensity of the fluorescent secondary antibody. Values are means ±SE. Grey cells mark significant differences *= P < 0.05, **= P < 0.01, ***= P < 0.001 (Student's *t* test, *n* = 5 biological replicates with pooled seedlings per replicate).

Antibody	CaCl ₂ soluble		CDTA		NaOH		Antibody binds
	Col-0	<i>gh43null</i>	Col-0	<i>gh43null</i>	Col-0	<i>gh43null</i>	
JIM5	0	0	42 ± 1.1	43 ± 1.7	0	0	Homogalacturonan
JIM7	60 ± 2.0	54 ± 3.2	91 ± 1.8	92 ± 3.5	0	0	Homogalacturonan
LM5	21 ± 0.4	20 ± 1.9	10 ± 0.6	13 ± 0.5*	19 ± 1.9	26 ± 0.8*	(1,4)-β-D-Gal4
LM6	13 ± 1.3	11 ± 1.5	16 ± 1.0	17 ± 0.4	28 ± 1.2	31 ± 0.6	(1,5)-α-L-Araf5
LM18	0	0	31 ± 0.9	34 ± 1.0*	0	0	Homogalacturonan
LM19	0	0	47 ± 0.5	46 ± 0.5	61 ± 5.1	60 ± 2.1	Homogalacturonan
LM20	35 ± 1.1	29 ± 2.0*	90 ± 2.0	87 ± 2.0	0	0	Homogalacturonan
RU1	0	0	46 ± 3.9	47 ± 1.5	43 ± 2.8	42 ± 1.0	Backbone of RG-I
RU2	10 ± 1.2	4 ± 1.6*	84 ± 6.1	88 ± 2.1	64 ± 2.5	69 ± 2.3	Backbone of RG-I
LM15	0	0	3 ± 1.7	8 ± 0.7*	73 ± 3.6	78 ± 3.0	XXXG-motif in xyloglucan
LM25	31 ± 0.6	30 ± 3.1	31 ± 2.0	34 ± 1.5	62 ± 1.5	71 ± 2.6*	XLLG, XLG, XXXG in xyloglucan
LM10	0	0	0	0	27 ± 1.4	25 ± 1.4	(1,4)-β-D-xylan
LM11	0	0	0	0	35 ± 1.7	35 ± 2.6	(1,4)-β-D-xylan
LM28	8 ± 0.8	8 ± 2.3	0	0	58 ± 3.9	51 ± 1.3	Glucuronosyl-containing epitope in heteroxylan
LM23	0	0	0	0	7 ± 1.9	9 ± 1.7	Non-acetylated xylosyl residues
BS400-4	0	0	0	0	28 ± 1.5	32 ± 1.9	(1,4)-β-D-mannan/galactomannan
CBM 3a	0	0	17 ± 5.8	24 ± 1.5	38 ± 1.4	44 ± 1.7*	Crystalline cellulose
LM1	12 ± 0.6	10 ± 1.0	0	0	0	0	Extensin
LM3	33 ± 1.6	28 ± 2.8	17 ± 0.7	18 ± 0.6	25 ± 2.3	30 ± 0.6	Extensin
JIM11	16 ± 2.4	10 ± 2.8	13 ± 0.6	13 ± 0.6	22 ± 2.4	28 ± 0.5	Extensin
JIM12	35 ± 1.8	32 ± 2.4	12 ± 0.4	10 ± 0.6	16 ± 2.0	20 ± 1.6	Extensin
JIM20	37 ± 2.2	31 ± 2.8	8 ± 0.8	10 ± 0.6	20 ± 2.2	26 ± 0.4*	Extensin
LM2	13 ± 1.2	8 ± 2.2	0	0	10 ± 0.9	15 ± 1.2*	GlcA terminally attached to 1,6-linked galactan
LM14	41 ± 1.9	39 ± 2.2	16 ± 1.1	17 ± 0.5	22 ± 1.1	29 ± 0.6***	AGP
JIM13	16 ± 1.0	12 ± 0.9*	6 ± 0.2	6 ± 0.3	8 ± 0.5	12 ± 1.0*	AGP
JIM16	32 ± 1.4	28 ± 1.8	0	0	0	0	β-1,3-linked galactan backbone substituted with a single β-1,6-linked Gal residue
MAC 207	35 ± 1.6	34 ± 1.7	12 ± 1.0	13 ± 0.8	11 ± 0.7	15 ± 0.9**	AGP

739

740

741 **Main Figure Legends**

742

743 **Figure 1. Characterisation of the *gh43* Arabidopsis T-DNA insertion lines.**

744 (A) Schematic diagram of the *GH43A* and *GH43B* gene structure and the T-DNA insertion
745 sites. The white and black boxes indicate untranslated and translated regions, respectively.

746 (B) Col-0 and *gh43* seedlings grown on nutrient media without sugar for 4 days and then
747 moved to media without sugar for 6 days. Scale bar = 5mm

748 (C) Col-0 and *gh43* seedlings grown on nutrient media without sugar for 4 days and then
749 moved to media with 4.5% glucose for 6 days. Scale bar = 5mm

750 (D) Root elongation of Col-0 and *gh43* seedlings grown on nutrient media without sugar for 4
751 days and then 6 days on media with 4.5% glucose. Values are means \pm SE ($n = 25 - 28$
752 biological replicates). Means not sharing a common letter are significantly different at $P <$
753 0.05, as determined by Tukey's test after one-way ANOVA.

754 (E) Root elongation of Col-0 and *gh43* seedlings grown on nutrient media without sugar for 4
755 days and then 6 days on media without glucose. Values are means \pm SE ($n = 25 - 28$ biological
756 replicates). Means not sharing a common letter are significantly different at $P < 0.05$, as
757 determined by Tukey's test after one-way ANOVA.

758 (F) Light microscopy images of Col-0 and *gh43null* root tip after seedlings were grown 4
759 days on nutrient media followed by 6 days on 4.5% glucose media. Scale bar = 100 μ m.

760 (G) Confocal laser scanning microscope images of Col-0 and *gh43null* roots stably expressing
761 the *LTI6a-GFP* plasma membrane marker. Images were obtained 10 hours after moving 4-day
762 old seedlings to nutrient media without (left) and with 4.5% glucose (right). Scale bars = 100
763 μ m.

764

765 **Figure 2. Co-localization of GH43A-YFP and GH43B-YFP with mCherry Golgi**
766 **markers.**

767 (A) Confocal laser scanning microscope images of root epidermis cells in Arabidopsis
768 seedlings stably expressing pGH43A::GH43A-cYFP or pGH43B::GH43B-cYFP and the cis-
769 Golgi marker SYP32-mCherry or the Trans Golgi Network (TGN) marker SYP43-mCherry.
770 Images were captured with a Zeiss LSM880 confocal microscope. Scale bars = 5 μ m.

771 (B) Degree of co-localization of pGH43A::GH43A-cYFP with SYP32-mCherry or SYP43-
772 mCherry in the root elongation zone epidermis. Images were captured from three independent
773 GH43A-cYFP lines (L1-L3) and five seedlings per line. The values represent the degree of
774 Pearson's correlation between the YFP and RFP channel.

775 (C) Degree of co-localization of pGH43B::GH43B-cYFP with SYP32-mCherry or SYP43-
776 mCherry in the root elongation zone epidermis. Images were captured from three independent
777 GH43A-cYFP lines (L1-L3) and five seedlings per line. The values represent the degree of
778 Pearson's correlation between the YFP and RFP channel.

779

780 **Figure 3. Thin layer chromatography (TLC) analysis of sugars released by recombinant**
781 **Arabidopsis GH43 activity.**

782 Hydrolytic activity of heterologous GH43A and GH43B against (1) Methyl β -D-
783 galactopyranosyl-(1 \rightarrow 3)- β -D-galactopyranoside, (2) Methyl β -D-galactopyranosyl-(1 \rightarrow 6)- β -
784 D-galactopyranoside, (3) Methyl β -D-galactopyranosyl-(1 \rightarrow 6)- β -D-galactopyranosyl-(1 \rightarrow 3)-
785 β -D-galactopyranoside and (4) Methyl β -D-galactopyranosyl-(1 \rightarrow 3)-[β -D-galactopyranosyl-
786 (1 \rightarrow 6)]- β -D-galactopyranoside. The digestion products were separated with TLC. Con=
787 substrate in buffer without enzyme, A = GH43A and B = GH43B.

788

789 **Figure 4. Spectrophotometric quantification of cell wall bound and soluble**
790 **arabinogalactan proteins with β -Yariv.**

791 (A) β -Yariv binding to wild type (Col-0) and *gh43null* cell walls from seven-day old
792 seedlings after removal of CaCl₂ and AIR1 soluble fractions. Amount of cell wall bound β -
793 Yariv was quantified against a Gum Arabic standard. Values are means \pm SE. *= P < 0.05
794 (unpaired *t* test, *n* = 5 biological replicate pools of seedlings).

795 (B) β -Yariv binding to the CaCl₂ soluble fraction from wild type (Col-0) and *gh43null* seven-
796 day old seedlings. Amount of bound β -Yariv was quantified against a Gum Arabic standard.
797 Values are means \pm SE. (*n* = 5 biological replicate pools of seedlings).

798

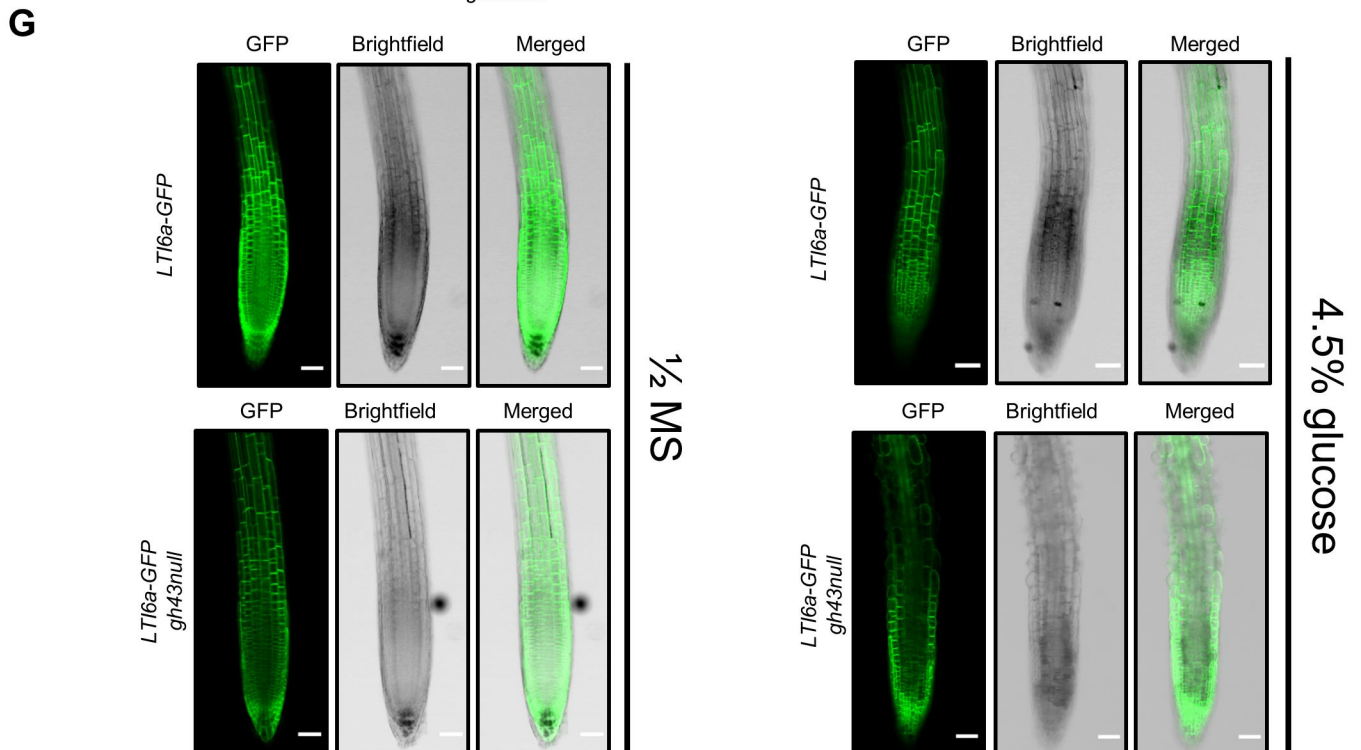
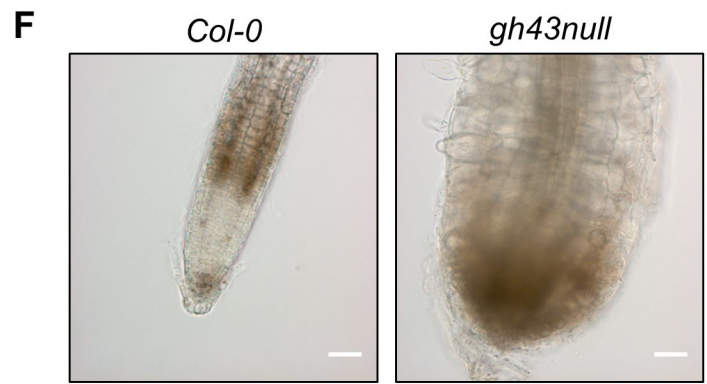
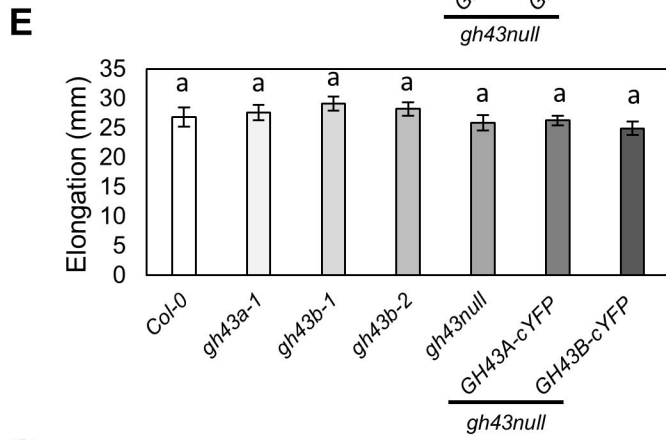
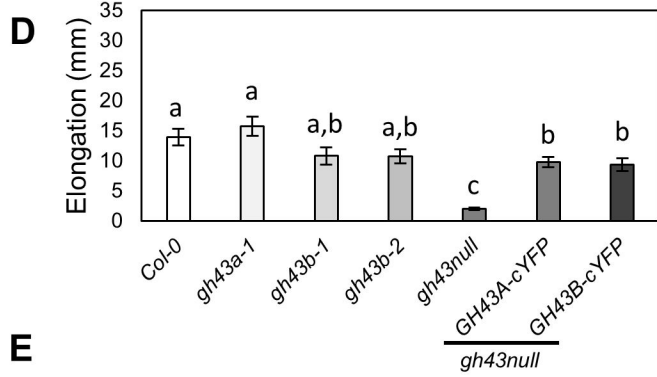
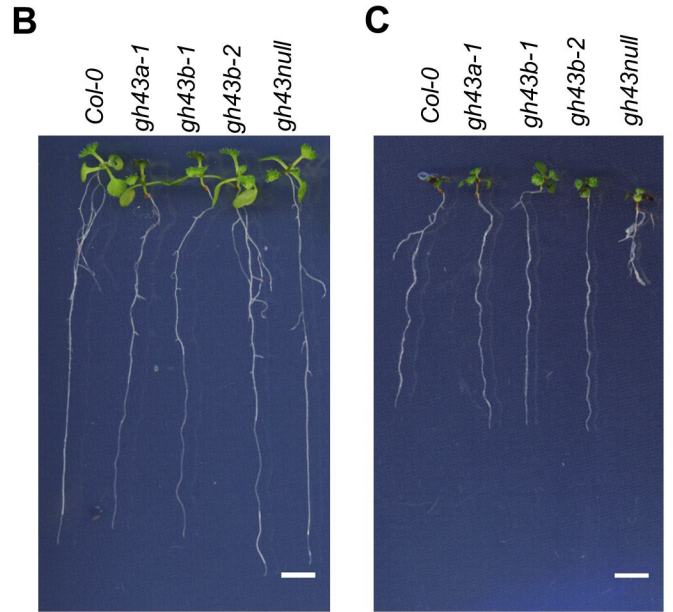
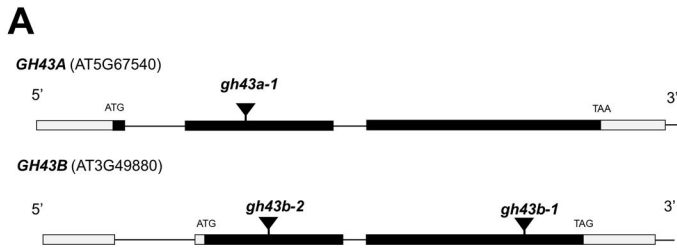


Figure 1. Characterisation of the *gh43* Arabidopsis T-DNA insertion lines.

(A) Schematic diagram of the GH43A and GH43B gene structure and the T-DNA insertion sites.

The white and black boxes indicate untranslated and translated regions, respectively.

(B) *Col-0* and *gh43* seedlings grown on nutrient media without sugar for 4 days and then moved to media without sugar for 6 days. Scale bar = 5mm

(C) *Col-0* and *gh43* seedlings grown on nutrient media without sugar for 4 days and then moved to media with 4.5% glucose for 6 days. Scale bar = 5mm

(D) Root elongation of *Col-0* and *gh43* seedlings grown on nutrient media without sugar for 4 days and then 6 days on media with 4.5% glucose. Values are means \pm SE (n = 25 – 28 biological replicates). Means not sharing a common letter are significantly different at P < 0.05, as determined by Tukey's test after one-way ANOVA.

(E) Root elongation of *Col-0* and *gh43* seedlings grown on nutrient media without sugar for 4 days and then 6 days on media without glucose. Values are means \pm SE (n = 25 – 28 biological replicates). Means not sharing a common letter are significantly different at P < 0.05, as determined by Tukey's test after one-way ANOVA.

(F) Light microscopy images of *Col-0* and *gh43null* root tip after seedlings were grown 4 days on nutrient media followed by 6 days on 4.5% glucose media. Scale bar = 100 μ m.

(G) Confocal laser scanning microscope images of *Col-0* and *gh43null* roots stably expressing the LTI6a-GFP plasma membrane marker. Images were obtained 10 hours after moving 4-day old seedlings to nutrient media without (left) and with 4.5% glucose (right). Scale bars = 100 μ m.

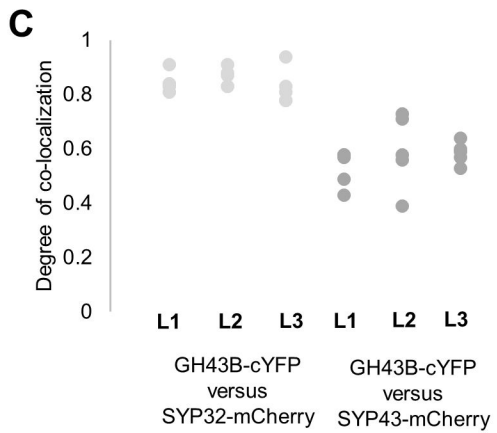
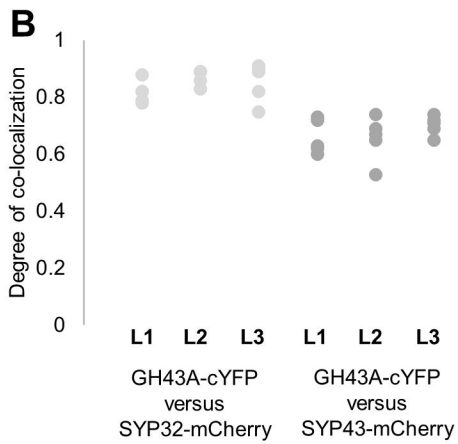
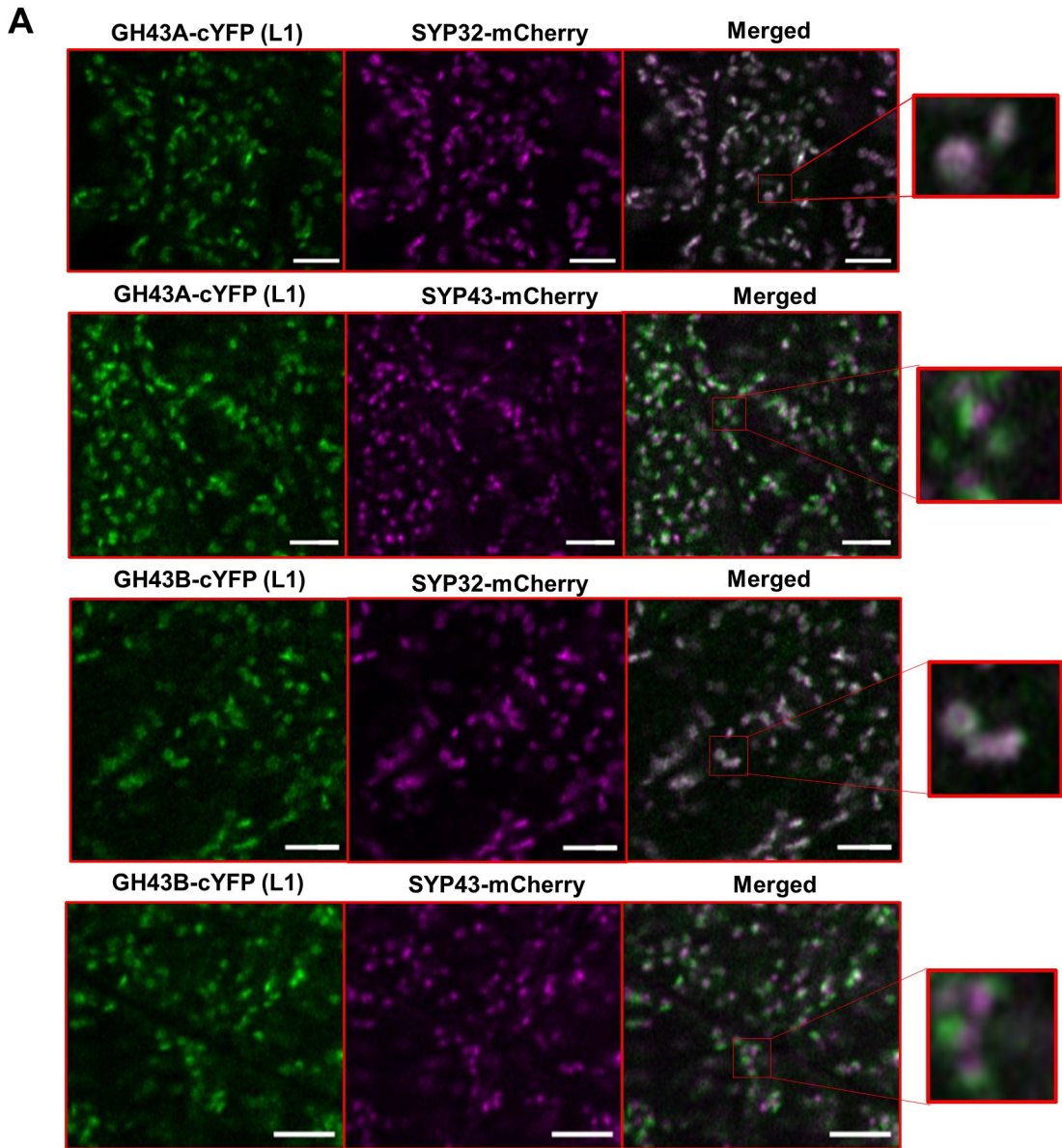
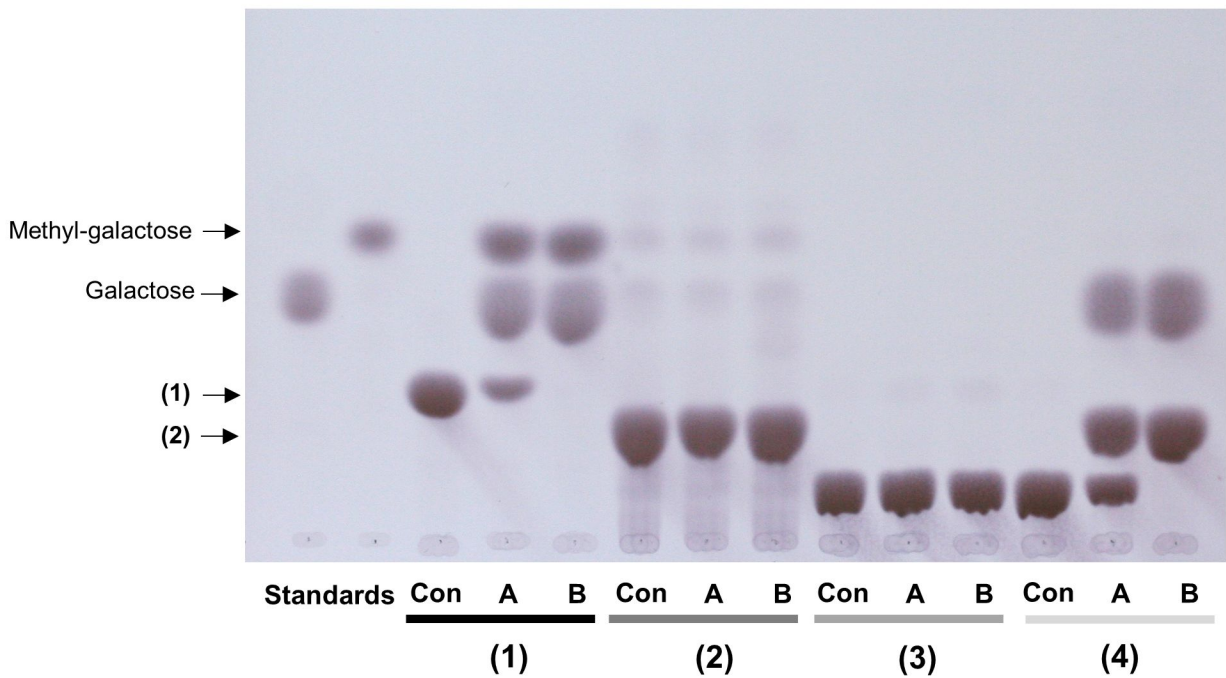


Figure 2. Co-localization of GH43A-YFP and GH43B-YFP with mCherry Golgi markers.

(A) Confocal laser scanning microscope images of root epidermis cells in Arabidopsis seedlings stably expressing pGH43A::GH43A-cYFP or pGH43B::GH43B-cYFP and the cis-Golgi marker SYP32-mCherry or the Trans Golgi Network (TGN) marker SYP43-mCherry. Images were captured with a Zeiss LSM880 confocal microscope. Scale bars = 5 μ m.

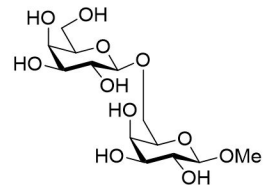
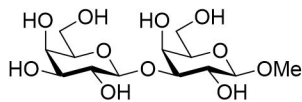
(B) Degree of co-localization of pGH43A::GH43A-cYFP with SYP32-mCherry or SYP43-mCherry in the root elongation zone epidermis. Images were captured from three independent GH43A-cYFP lines (L1-L3) and five seedlings per line. The values represent the degree of Pearson's correlation between the YFP and RFP channel.

(C) Degree of co-localization of pGH43B::GH43B-cYFP with SYP32-mCherry or SYP43-mCherry in the root elongation zone epidermis. Images were captured from three independent GH43A-cYFP lines (L1-L3) and five seedlings per line. The values represent the degree of Pearson's correlation between the YFP and RFP channel.



(1) β -D-Galp-(1 \rightarrow 3)- β -D-GalpOMe

(2) β -D-Galp-(1 \rightarrow 6)- β -D-GalpOMe



(3) β -D-Galp-(1 \rightarrow 6)- β -D-Galp-(1 \rightarrow 3)- β -D-GalpOMe

(4) β -D-Galp-(1 \rightarrow 3)-[β -D-Galp-(1 \rightarrow 6)]- β -D-GalpOMe

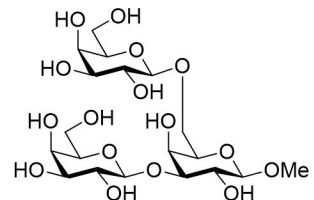
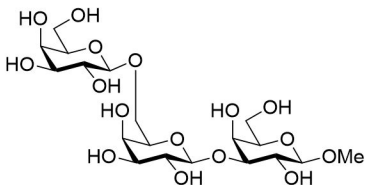


Figure 3. Thin layer chromatography (TLC) analysis of sugars released by recombinant Arabidopsis GH43 activity.

Hydrolytic activity of heterologous GH43A and GH43B against (1) Methyl β -D-galactopyranosyl-(1 \rightarrow 3)- β -D-galactopyranoside, (2) Methyl β -D-galactopyranosyl-(1 \rightarrow 6)- β -D-galactopyranoside, (3) Methyl β -D-galactopyranosyl-(1 \rightarrow 6)- β -D-galactopyranosyl-(1 \rightarrow 3)- β -D-galactopyranoside and (4) Methyl β -D-galactopyranosyl-(1 \rightarrow 3)-[β -D-galactopyranosyl-(1 \rightarrow 6)]- β -D-galactopyranoside. The digestion products were separated with TLC. Con= substrate in buffer without enzyme. A = GH43A and B = GH43B.

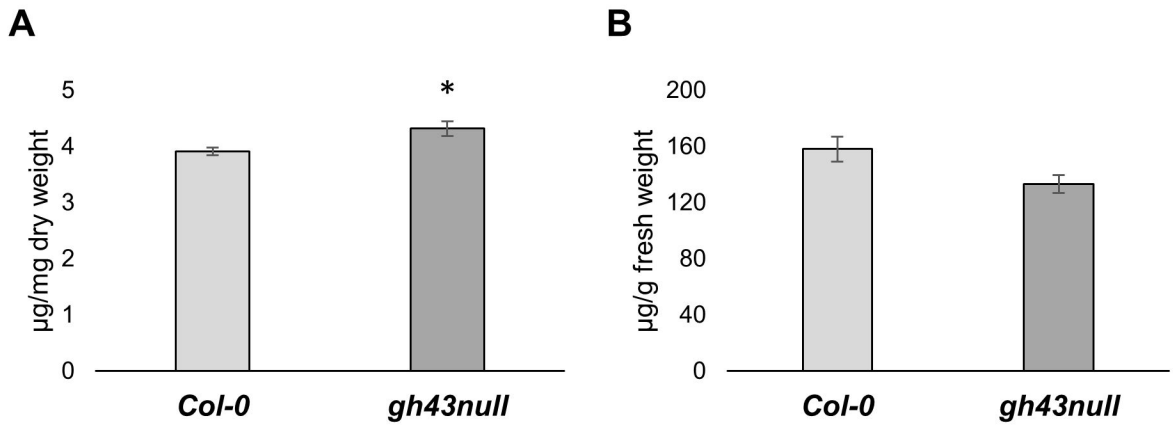


Figure 4. Spectrophotometric quantification of cell wall bound and soluble arabinogalactan proteins with β -Yariv.

(A) β -Yariv binding to wild type (*Col-0*) and *gh43null* cell walls from seven-day old seedlings after removal of CaCl_2 and AIR1 soluble fractions. Amount of cell wall bound β -Yariv was quantified against a Gum Arabic standard. Values are means \pm SE. *= $P < 0.05$ (unpaired t test, $n = 5$ biological replicate pools of seedlings).

(B) β -Yariv binding to the CaCl_2 soluble fraction from wild type (*Col-0*) and *gh43null* seven-day old seedlings. Amount of bound β -Yariv was quantified against a Gum Arabic standard. Values are means \pm SE. ($n = 5$ biological replicate pools of seedlings).

Parsed Citations

We would like to thank Mikael Lindberg from the Umeå University Protein Expertise Platform (PEP), for help with expressing the recombinant Arabidopsis GH43s. We would like to thank Dr. Junko Takahashi-Schmidt and the UPSC Biopolymer Analytical Platform for help with the cell wall monosugar analysis. This work was supported by The Swedish Foundation for Strategic Research (Value Tree), Bio4Energy (Swedish Programme for Renewable Energy), the UPSC Centre for Forest Biotechnology funded by VINNOVA and the Swedish Research Council for Sustainable Development (Formas).

Author Contribution

P.N., B.P., M.S.M., B.J. and P.U. planned and performed experiments and analyzed data. T.N. planned experiments and analyzed data. P.N. and T.N. wrote the manuscript with help from the other authors.

Literature

Akiyama Y, Eda S, Kato K (1984) Gum Arabic Is a Kind of Arabinogalactan Protein. Agricultural and Biological Chemistry 48: 235-237

Pubmed: [Author and Title](#)

Google Scholar: [Author Only](#) [Title Only](#) [Author and Title](#)

Bashline L, Lei L, Li SD, Gu Y (2014) Cell Wall, Cytoskeleton, and Cell Expansion in Higher Plants. Molecular Plant 7: 586-600

Pubmed: [Author and Title](#)

Google Scholar: [Author Only](#) [Title Only](#) [Author and Title](#)

Basu D, Tian L, Wang W, Bobbs S, Herock H, Travers A, Showalter AM (2015) A small multigene hydroxyproline-O-galactosyltransferase family functions in arabinogalactan-protein glycosylation, growth and development in Arabidopsis. BMC Plant Biol 15: 295

Pubmed: [Author and Title](#)

Google Scholar: [Author Only](#) [Title Only](#) [Author and Title](#)

Basu D, Wang W, Ma S, DeBrosse T, Poirier E, Emch K, Soukup E, Tian L, Showalter AM (2015) Two Hydroxyproline Galactosyltransferases, GALT5 and GALT2, Function in Arabinogalactan-Protein Glycosylation, Growth and Development in Arabidopsis. PLoS One 10: e0125624

Pubmed: [Author and Title](#)

Google Scholar: [Author Only](#) [Title Only](#) [Author and Title](#)

Benfey PN, Linstead PJ, Roberts K, Schiefelbein JW, Hauser MT, Aeschbacher RA (1993) Root development in Arabidopsis: four mutants with dramatically altered root morphogenesis. Development 119: 57-70

Pubmed: [Author and Title](#)

Google Scholar: [Author Only](#) [Title Only](#) [Author and Title](#)

Cosgrove DJ (2005) Growth of the plant cell wall. Nat Rev Mol Cell Biol 6: 850-861

Pubmed: [Author and Title](#)

Google Scholar: [Author Only](#) [Title Only](#) [Author and Title](#)

Cosgrove DJ (2014) Re-constructing our models of cellulose and primary cell wall assembly. Current Opinion in Plant Biology 22: 122-131

Pubmed: [Author and Title](#)

Google Scholar: [Author Only](#) [Title Only](#) [Author and Title](#)

Dilokpimol A, Poulsen CP, Vereb G, Kaneko S, Schulz A, Geshi N (2014) Galactosyltransferases from Arabidopsis thaliana in the biosynthesis of type II arabinogalactan: molecular interaction enhances enzyme activity. BMC Plant Biol 14: 90

Pubmed: [Author and Title](#)

Google Scholar: [Author Only](#) [Title Only](#) [Author and Title](#)

Du H, Clarke AE, Bacic A (1996) Arabinogalactan-proteins: a class of extracellular matrix proteoglycans involved in plant growth and development. Trends Cell Biol 6: 411-414

Pubmed: [Author and Title](#)

Google Scholar: [Author Only](#) [Title Only](#) [Author and Title](#)

Ellis M, Egelund J, Schultz CJ, Bacic A (2010) Arabinogalactan-proteins: key regulators at the cell surface? Plant Physiol 153: 403-419

Pubmed: [Author and Title](#)

Google Scholar: [Author Only](#) [Title Only](#) [Author and Title](#)

Geldner N, Denervaud-Tendon V, Hyman DL, Mayer U, Stierhof YD, Chory J (2009) Rapid, combinatorial analysis of membrane compartments in intact plants with a multicolor marker set. Plant Journal 59: 169-178

Pubmed: [Author and Title](#)

Google Scholar: [Author Only](#) [Title Only](#) [Author and Title](#)

Geshi N, Johansen JN, Dilokpimol A, Rolland A, Belcram K, Verger S, Kotake T, Tsumuraya Y, Kaneko S, Tryfona T, Dupree P, Scheller HV, Hofte H, Mouille G (2013) A galactosyltransferase acting on arabinogalactan protein glycans is essential for embryo development in Arabidopsis. Plant Journal 76: 128-137

Pubmed: [Author and Title](#)

Google Scholar: [Author Only](#) [Title Only](#) [Author and Title](#)

Gille S, Sharma V, Baidoo EEK, Keasling JD, Scheller HV, Pauly M (2013) Arabinosylation of a Yariv-Precipitable Cell Wall Polymer

Impacts Plant Growth as Exemplified by the Arabidopsis Glycosyltransferase Mutant ray1. Molecular Plant 6: 1369-1372

Pubmed: [Author and Title](#)

Google Scholar: [Author Only Title Only Author and Title](#)

Grebe M, Xu J, Mobius W, Ueda T, Nakano A, Geuze HJ, Rook MB, Scheres B (2003) Arabidopsis sterol endocytosis involves actin-mediated trafficking via ARAG-positive early endosomes. Curr Biol 13: 1378-1387

Pubmed: [Author and Title](#)

Google Scholar: [Author Only Title Only Author and Title](#)

Gu Y, Kaplinsky N, Bringmann M, Cobb A, Carroll A, Sampathkumar A, Baskin TI, Persson S, Somerville CR (2010) Identification of a cellulose synthase-associated protein required for cellulose biosynthesis. Proceedings of the National Academy of Sciences of the United States of America 107: 12866-12871

Pubmed: [Author and Title](#)

Google Scholar: [Author Only Title Only Author and Title](#)

Gunl M, Neumetzler L, Kraemer F, de Souza A, Schultink A, Pena M, York WS, Pauly M (2011) AXY8 encodes an alpha-fucosidase, underscoring the importance of apoplastic metabolism on the fine structure of Arabidopsis cell wall polysaccharides. Plant Cell 23: 4025-4040

Pubmed: [Author and Title](#)

Google Scholar: [Author Only Title Only Author and Title](#)

Gunl M, Pauly M (2011) AXY3 encodes a alpha-xylosidase that impacts the structure and accessibility of the hemicellulose xyloglucan in Arabidopsis plant cell walls. Planta 233: 707-719

Pubmed: [Author and Title](#)

Google Scholar: [Author Only Title Only Author and Title](#)

Haque M, Kotake T, Tsumuraya Y (2005) Mode of action of beta-glucuronidase from Aspergillus niger on the sugar chains of arabinogalactan-protein. Biosci Biotechnol Biochem 69: 2170-2177

Pubmed: [Author and Title](#)

Google Scholar: [Author Only Title Only Author and Title](#)

Harholt J, Sorensen I, Fangel J, Roberts A, Willats WGT, Scheller HV, Petersen BL, Banks A, Ulvskov P (2012) The Glycosyltransferase Repertoire of the Spikemoss Selaginella moellendorffii and a Comparative Study of Its Cell Wall. Plos One 7

Pubmed: [Author and Title](#)

Google Scholar: [Author Only Title Only Author and Title](#)

Harholt J, Suttangkakul A, Vibe Scheller H (2010) Biosynthesis of pectin. Plant Physiol 153: 384-395

Pubmed: [Author and Title](#)

Google Scholar: [Author Only Title Only Author and Title](#)

Hauser MT, Morikami A, Benfey PN (1995) Conditional root expansion mutants of Arabidopsis. Development 121: 1237-1252

Pubmed: [Author and Title](#)

Google Scholar: [Author Only Title Only Author and Title](#)

Hernandez-Gomez MC, Rydahl MG, Rogowski A, Morland C, Cartmell A, Crouch L, Labourel A, Fontes CM, Willats WG, Gilbert HJ, Knox JP (2015) Recognition of xyloglucan by the crystalline cellulose-binding site of a family 3a carbohydrate-binding module. FEBS Lett 589: 2297-2303

Pubmed: [Author and Title](#)

Google Scholar: [Author Only Title Only Author and Title](#)

Hijazi M, Velasquez SM, Jamet E, Estevez JM, Albenne C (2014) An update on post-translational modifications of hydroxyproline-rich glycoproteins: toward a model highlighting their contribution to plant cell wall architecture. Front Plant Sci 5: 395

Pubmed: [Author and Title](#)

Google Scholar: [Author Only Title Only Author and Title](#)

Höfte H, Peaucelle A, Braybrook S (2012) Cell wall mechanics and growth control in plants: the role of pectins revisited. Frontiers in plant science 3: 121

Pubmed: [Author and Title](#)

Google Scholar: [Author Only Title Only Author and Title](#)

Ichinose H, Kuno A, Kotake T, Yoshida M, Sakka K, Hirabayashi J, Tsumuraya Y, Kaneko S (2006) Characterization of an exo-beta-1,3-galactanase from Clostridium thermocellum. Appl Environ Microbiol 72: 3515-3523

Pubmed: [Author and Title](#)

Google Scholar: [Author Only Title Only Author and Title](#)

Ichinose H, Yoshida M, Kotake T, Kuno A, Igarashi K, Tsumuraya Y, Samejima M, Hirabayashi J, Kobayashi H, Kaneko S (2005) An exo-beta-1,3-galactanase having a novel beta-1,3-galactan-binding module from Phanerochaete chrysosporium. J Biol Chem 280: 25820-25829

Pubmed: [Author and Title](#)

Google Scholar: [Author Only Title Only Author and Title](#)

Jiang D, Fan J, Wang X, Zhao Y, Huang B, Liu J, Zhang XC (2012) Crystal structure of 1,3Gal43A, an exo-beta-1,3-galactanase from Clostridium thermocellum. J Struct Biol 180: 447-457

Pubmed: [Author and Title](#)

Google Scholar: [Author Only Title Only Author and Title](#)

Jones L, Seymour GB, Knox JP (1997) Localization of pectic galactan in tomato cell walls using a monoclonal antibody specific to (1-4)-beta-D-galactan. *Plant Physiology* 113: 1405-1412

Pubmed: [Author and Title](#)

Google Scholar: [Author Only](#) [Title Only](#) [Author and Title](#)

Jordan DB, Wagschal K, Grigorescu AA, Braker JD (2013) Highly active beta-xylosidases of glycoside hydrolase family 43 operating on natural and artificial substrates. *Appl Microbiol Biotechnol* 97: 4415-4428

Pubmed: [Author and Title](#)

Google Scholar: [Author Only](#) [Title Only](#) [Author and Title](#)

Keegstra K, Talmadge KW, Bauer W, Albersheim P (1973) The structure of plant cell walls: III. A model of the walls of suspension-cultured sycamore cells based on the interconnections of the macromolecular components. *Plant physiology* 51: 188-197

Pubmed: [Author and Title](#)

Google Scholar: [Author Only](#) [Title Only](#) [Author and Title](#)

Kitazawa K, Tryfona T, Yoshimi Y, Hayashi Y, Kawauchi S, Antonov L, Tanaka H, Takahashi T, Kaneko S, Dupree P, Tsumuraya Y, Kotake T (2013) beta-galactosyl Yariv reagent binds to the beta-1,3-galactan of arabinogalactan proteins. *Plant Physiol* 161: 1117-1126

Pubmed: [Author and Title](#)

Google Scholar: [Author Only](#) [Title Only](#) [Author and Title](#)

Knoch E, Dilokpimol A, Tryfona T, Poulsen CP, Xiong GY, Harholt J, Petersen BL, Ulvskov P, Hadi MZ, Kotake T, Tsumuraya Y, Pauly M, Dupree P, Geshi N (2013) A beta-glucuronosyltransferase from *Arabidopsis thaliana* involved in biosynthesis of type II arabinogalactan has a role in cell elongation during seedling growth. *Plant Journal* 76: 1016-1029

Pubmed: [Author and Title](#)

Google Scholar: [Author Only](#) [Title Only](#) [Author and Title](#)

Kotake T, Kitazawa K, Takata R, Okabe K, Ichinose H, Kaneko S, Tsumuraya Y (2009) Molecular cloning and expression in *Pichia pastoris* of a *Irpex lacteus* exo-beta-(1-->3)-galactanase gene. *Biosci Biotechnol Biochem* 73: 2303-2309

Pubmed: [Author and Title](#)

Google Scholar: [Author Only](#) [Title Only](#) [Author and Title](#)

Kubo M, Udagawa M, Nishikubo N, Horiguchi G, Yamaguchi M, Ito J, Mimura T, Fukuda H, Demura T (2005) Transcription switches for protoxylem and metaxylem vessel formation. *Genes Dev* 19: 1855-1860

Pubmed: [Author and Title](#)

Google Scholar: [Author Only](#) [Title Only](#) [Author and Title](#)

Lampert DT (2013) Preparation of arabinogalactan glycoproteins from plant tissue. *Bioprotocol* 3: 1-5

Pubmed: [Author and Title](#)

Google Scholar: [Author Only](#) [Title Only](#) [Author and Title](#)

Latha Gandla M, Derba-Maceluch M, Liu X, Gerber L, Master ER, Mellerowicz EJ, Jonsson LJ (2015) Expression of a fungal glucuronoyl esterase in *Populus*: effects on wood properties and saccharification efficiency. *Phytochemistry* 112: 210-220

Pubmed: [Author and Title](#)

Google Scholar: [Author Only](#) [Title Only](#) [Author and Title](#)

Liebinger E, Huttner S, Vavra U, Fischl R, Schoberer J, Grass J, Blaukopf C, Seifert GJ, Altmann F, Mach L, Strasser R (2009) Class I alpha-mannosidases are required for N-glycan processing and root development in *Arabidopsis thaliana*. *Plant Cell* 21: 3850-3867

Pubmed: [Author and Title](#)

Google Scholar: [Author Only](#) [Title Only](#) [Author and Title](#)

Ljung K, Nemhauser JL, Perata P (2015) New mechanistic links between sugar and hormone signalling networks. *Current Opinion in Plant Biology* 25: 130-137

Pubmed: [Author and Title](#)

Google Scholar: [Author Only](#) [Title Only](#) [Author and Title](#)

Marcus SE, Verhertbruggen Y, Herve C, Ordaz-Ortiz JJ, Farkas V, Pedersen HL, Willats WG, Knox JP (2008) Pectic homogalacturonan masks abundant sets of xyloglucan epitopes in plant cell walls. *BMC Plant Biol* 8: 60

Pubmed: [Author and Title](#)

Google Scholar: [Author Only](#) [Title Only](#) [Author and Title](#)

McCleary BV, McKie VA, Draga A, Rooney E, Mangan D, Larkin J (2015) Hydrolysis of wheat flour arabinoxylan, acid-debranched wheat flour arabinoxylan and arabino-xylo-oligosaccharides by beta-xylanase, alpha-L-arabinofuranosidase and beta-xylosidase. *Carbohydr Res* 407: 79-96

Pubmed: [Author and Title](#)

Google Scholar: [Author Only](#) [Title Only](#) [Author and Title](#)

Mewis K, Lenfant N, Lombard V, Henrissat B (2016) Dividing the Large Glycoside Hydrolase Family 43 into Subfamilies: a Motivation for Detailed Enzyme Characterization. *Appl Environ Microbiol* 82: 1686-1692

Pubmed: [Author and Title](#)

Google Scholar: [Author Only](#) [Title Only](#) [Author and Title](#)

Mohnen D (2008) Pectin structure and biosynthesis. *Curr Opin Plant Biol* 11: 266-277

Pubmed: [Author and Title](#)

Google Scholar: [Author Only](#) [Title Only](#) [Author and Title](#)

Moller IE, Pettolino FA, Hart C, Lampugnani ER, Willats WGT, Bacic A (2012) Glycan Profiling of Plant Cell Wall Polymers using Microarrays. Jove-Journal of Visualized Experiments

Pubmed: [Author and Title](#)

Google Scholar: [Author Only Title Only Author and Title](#)

Niittyla T, Fuglsang AT, Palmgren MG, Frommer WB, Schulze WX (2007) Temporal analysis of sucrose-induced phosphorylation changes in plasma membrane proteins of Arabidopsis. Mol Cell Proteomics 6: 1711-1726

Pubmed: [Author and Title](#)

Google Scholar: [Author Only Title Only Author and Title](#)

Ogawa-Ohnishi M, Matsubayashi Y (2015) Identification of three potent hydroxyproline O-galactosyltransferases in Arabidopsis. Plant J 81: 736-746

Pubmed: [Author and Title](#)

Google Scholar: [Author Only Title Only Author and Title](#)

Parsons HT, Christiansen K, Knierim B, Carroll A, Ito J, Batth TS, Smith-Moritz AM, Morrison S, McInerney P, Hadi MZ, Auer M, Mukhopadhyay A, Petzold CJ, Scheller HV, Loque D, Heazlewood JL (2012) Isolation and proteomic characterization of the Arabidopsis Golgi defines functional and novel components involved in plant cell wall biosynthesis. Plant Physiol 159: 12-26

Pubmed: [Author and Title](#)

Google Scholar: [Author Only Title Only Author and Title](#)

Parsons HT, Stevens TJ, McFarlane HE, Vidal-Melgosa S, Griss J, Lawrence N, Butler R, Sousa MML, Salemi M, Willats WGT, Petzold CJ, Heazlewood JL, Lilley KS (2019) Separating Golgi proteins from cis to trans reveals underlying properties of cisternal localization. Plant Cell

Pubmed: [Author and Title](#)

Google Scholar: [Author Only Title Only Author and Title](#)

Pennell RI, Janniche L, Kjellbom P, Scofield GN, Peart JM, Roberts K (1991) Developmental Regulation of a Plasma-Membrane Arabinogalactan Protein Epitope in Oilseed Rape Flowers. Plant Cell 3: 1317-1326

Pubmed: [Author and Title](#)

Google Scholar: [Author Only Title Only Author and Title](#)

Ralet MC, Tranquet O, Poulain D, Moise A, Guillon F (2010) Monoclonal antibodies to rhamnogalacturonan I backbone. Planta 231: 1373-1383

Pubmed: [Author and Title](#)

Google Scholar: [Author Only Title Only Author and Title](#)

Rende U, Wang W, Gandla ML, Jonsson LJ, Niittyla T (2016) Cytosolic invertase contributes to the supply of substrate for cellulose biosynthesis in developing wood. New Phytol

Pubmed: [Author and Title](#)

Google Scholar: [Author Only Title Only Author and Title](#)

Rose JKC, Lee SJ (2010) Straying off the Highway: Trafficking of Secreted Plant Proteins and Complexity in the Plant Cell Wall Proteome. Plant Physiology 153: 433-436

Pubmed: [Author and Title](#)

Google Scholar: [Author Only Title Only Author and Title](#)

Ruprecht C, Bartetzko MP, Senf D, Dallabernadina P, Boos I, Andersen MCF, Kotake T, Knox JP, Hahn MG, Clausen MH, Pfengle F (2017) A Synthetic Glycan Microarray Enables Epitope Mapping of Plant Cell Wall Glycan-Directed Antibodies. Plant Physiol 175: 1094-1104

Pubmed: [Author and Title](#)

Google Scholar: [Author Only Title Only Author and Title](#)

Sanchez-Rodriguez C, Bauer S, Hematy K, Saxe F, Ibanez AB, Vodermaier V, Konlechner C, Sampathkumar A, Ruggeberg M, Aichinger E, Neumetzler L, Burgert I, Somerville C, Hauser MT, Persson S (2012) Chitinase-like1/pom-pom1 and its homolog CTL2 are glucan-interacting proteins important for cellulose biosynthesis in Arabidopsis. Plant Cell 24: 589-607

Pubmed: [Author and Title](#)

Google Scholar: [Author Only Title Only Author and Title](#)

Scheller HV, Ulvskov P (2010) Hemicelluloses. Annu Rev Plant Biol 61: 263-289

Pubmed: [Author and Title](#)

Google Scholar: [Author Only Title Only Author and Title](#)

Schindelman G, Morikami A, Jung J, Baskin TI, Carpita NC, Derbyshire P, McCann MC, Benfey PN (2001) COBRA encodes a putative GPI-anchored protein, which is polarly localized and necessary for oriented cell expansion in Arabidopsis. Genes & development 15: 1115-1127

Pubmed: [Author and Title](#)

Google Scholar: [Author Only Title Only Author and Title](#)

Showalter AM (1993) Structure and function of plant cell wall proteins. Plant Cell 5: 9-23

Pubmed: [Author and Title](#)

Google Scholar: [Author Only Title Only Author and Title](#)

Showalter AM, Basu D (2016) Extensin and Arabinogalactan-Protein Biosynthesis: Glycosyltransferases, Research Challenges, and

Biosensors. Front Plant Sci 7: 814

Pubmed: [Author and Title](#)

Google Scholar: [Author Only Title Only Author and Title](#)

Showalter AM, Keppler B, Lichtenberg J, Gu D, Welch LR (2010) A bioinformatics approach to the identification, classification, and analysis of hydroxyproline-rich glycoproteins. Plant Physiol 153: 485-513

Pubmed: [Author and Title](#)

Google Scholar: [Author Only Title Only Author and Title](#)

Smallwood M, Beven A, Donovan N, Neill SJ, Peart J, Roberts K, Knox JP (1994) Localization of Cell-Wall Proteins in Relation to the Developmental Anatomy of the Carrot Root Apex. Plant Journal 5: 237-246

Pubmed: [Author and Title](#)

Google Scholar: [Author Only Title Only Author and Title](#)

Smallwood M, Yates EA, Willats WGT, Martin H, Knox JP (1996) Immunochemical comparison of membrane-associated and secreted arabinogalactan-proteins in rice and carrot. Planta 198: 452-459

Pubmed: [Author and Title](#)

Google Scholar: [Author Only Title Only Author and Title](#)

Suzuki T, Narciso JO, Zeng W, van de Meene A, Yasutomi M, Takemura S, Lampugnani ER, Doblin MS, Bacic A, Ishiguro S (2017) KNS4/UPEX1: A Type II Arabinogalactan beta-(1,3)-Galactosyltransferase Required for Pollen Exine Development. Plant Physiol 173: 183-205

Pubmed: [Author and Title](#)

Google Scholar: [Author Only Title Only Author and Title](#)

Tan L, Eberhard S, Pattathil S, Warder C, Glushka J, Yuan C, Hao Z, Zhu X, Avci U, Miller JS, Baldwin D, Pham C, Orlando R, Darvill A, Hahn MG, Kieliszewski MJ, Mohnen D (2013) An Arabidopsis cell wall proteoglycan consists of pectin and arabinoxylan covalently linked to an arabinogalactan protein. Plant Cell 25: 270-287

Pubmed: [Author and Title](#)

Google Scholar: [Author Only Title Only Author and Title](#)

Tan L, Qiu F, Lampport DTA, Kieliszewski MJ (2004) Structure of a hydroxyproline (Hyp)-arabinogalactan polysaccharide from repetitive Ala-Hyp expressed in transgenic Nicotiana tabacum. Journal of Biological Chemistry 279: 13156-13165

Pubmed: [Author and Title](#)

Google Scholar: [Author Only Title Only Author and Title](#)

Tan L, Varnai P, Lampport DT, Yuan C, Xu J, Qiu F, Kieliszewski MJ (2010) Plant O-hydroxyproline arabinogalactans are composed of repeating trigalactosyl subunits with short bifurcated side chains. J Biol Chem 285: 24575-24583

Pubmed: [Author and Title](#)

Google Scholar: [Author Only Title Only Author and Title](#)

Tryfona T, Liang HC, Kotake T, Kaneko S, Marsh J, Ichinose H, Lovegrove A, Tsumuraya Y, Shewry PR, Stephens E, Dupree P (2010) Carbohydrate structural analysis of wheat flour arabinogalactan protein. Carbohydrate Research 345: 2648-2656

Pubmed: [Author and Title](#)

Google Scholar: [Author Only Title Only Author and Title](#)

Tryfona T, Liang HC, Kotake T, Tsumuraya Y, Stephens E, Dupree P (2012) Structural characterization of Arabidopsis leaf arabinogalactan polysaccharides. Plant Physiol 160: 653-666

Pubmed: [Author and Title](#)

Google Scholar: [Author Only Title Only Author and Title](#)

Tryfona T, Theys TE, Wagner T, Stott K, Keegstra K, Dupree P (2014) Characterisation of FUT4 and FUT6 alpha-(1 -> 2)-Fucosyltransferases Reveals that Absence of Root Arabinogalactan Fucosylation Increases Arabidopsis Root Growth Salt Sensitivity. Plos One 9

Pubmed: [Author and Title](#)

Google Scholar: [Author Only Title Only Author and Title](#)

Uemura T, Ueda T, Ohniwa RL, Nakano A, Takeyasu K, Sato MH (2004) Systematic analysis of SNARE molecules in Arabidopsis: dissection of the post-Golgi network in plant cells. Cell Struct Funct 29: 49-65

Pubmed: [Author and Title](#)

Google Scholar: [Author Only Title Only Author and Title](#)

Updegraff DM (1969) Semimicro determination of cellulose in biological materials. Anal Biochem 32: 420-424

Pubmed: [Author and Title](#)

Google Scholar: [Author Only Title Only Author and Title](#)

Verhertbruggen Y, Marcus SE, Haeger A, Ordaz-Ortiz JJ, Knox JP (2009) An extended set of monoclonal antibodies to pectic homogalacturonan. Carbohydr Res 344: 1858-1862

Pubmed: [Author and Title](#)

Google Scholar: [Author Only Title Only Author and Title](#)

Wang T, Park YB, Cosgrove DJ, Hong M (2015) Cellulose-Pectin Spatial Contacts Are Inherent to Never-Dried Arabidopsis Primary Cell Walls: Evidence from Solid-State Nuclear Magnetic Resonance. Plant Physiol 168: 871-884

Pubmed: [Author and Title](#)

Google Scholar: [Author Only](#) [Title Only](#) [Author and Title](#)

Wu Y, Williams M, Bernard S, Driouch A, Showalter AM, Faik A (2010) Functional identification of two nonredundant Arabidopsis alpha(1,2)fucosyltransferases specific to arabinogalactan proteins. J Biol Chem 285: 13638-13645

Pubmed: [Author and Title](#)

Google Scholar: [Author Only](#) [Title Only](#) [Author and Title](#)

Xue H, Veit C, Abas L, Tryfona T, Maresch D, Ricardi MM, Estevez JM, Strasser R, Seifert GJ (2017) Arabidopsis thaliana FLA4 functions as a glycan-stabilized soluble factor via its carboxy-proximal Fasciclin 1 domain. The Plant Journal 91: 613-630

Pubmed: [Author and Title](#)

Google Scholar: [Author Only](#) [Title Only](#) [Author and Title](#)

Yapo BM (2011) Rhamnogalacturonan-I: a structurally puzzling and functionally versatile polysaccharide from plant cell walls and mucilages. Polymer Reviews 51: 391-413

Pubmed: [Author and Title](#)

Google Scholar: [Author Only](#) [Title Only](#) [Author and Title](#)

Yates EA, Valdor JF, Haslam SM, Morris HR, Dell A, Mackie W, Knox JP (1996) Characterization of carbohydrate structural features recognized by anti-arabinogalactan-protein monoclonal antibodies. Glycobiology 6: 131-139

Pubmed: [Author and Title](#)

Google Scholar: [Author Only](#) [Title Only](#) [Author and Title](#)

Yeats TH, Sorek H, Wemmer DE, Somerville CR (2016) Cellulose Deficiency Is Enhanced on Hyper Accumulation of Sucrose by a H⁺-Coupled Sucrose Symporter. Plant Physiology 171: 110-124

Pubmed: [Author and Title](#)

Google Scholar: [Author Only](#) [Title Only](#) [Author and Title](#)